Scalar and Spinor Perturbation to the Kerr-NUT Space-time

Banibrata Mukhopadhyay* & Naresh Dadhich
Inter-University Centre for Astronomy and Astrophysics, Post Bag 4, Ganeshkhind, Pune-411007, India

We study the scalar and spinor perturbation, namely the Klein-Gordan and Dirac equations, in the Kerr-NUT space-time. The metric is invariant under the duality transformation involving the exchange of mass and NUT parameters on one hand and radial and angle coordinates on the other. We show that this invariance is also shared by the scalar and spinor perturbation equations. Further, by the duality transformation, one can go from the Kerr to the dual Kerr solution, and vice versa, and the same applies to the perturbation equations. In particular, it turns out that the potential barriers felt by the incoming scalar and spinor fields are higher for the dual Kerr than that for the Kerr. We also comment on existence of horizon and singularity.

KEY WORDS : Kerr-NUT space-time, metric perturbation, potential barrier

PACS NO. : 03.50.De, 04.20.-q, 04.70.-s, 95.30.Sf

I. INTRODUCTION

For asymptotically flat axially symmetric stationary electro-vacuum space-time, it is well known that the Kerr family is unique [1]. On relaxing the condition of asymptotic flatness, there occurs the NUT generalization of it, the Kerr-NUT family [2–4]. It has recently been shown [5] that this family is also unique for the space-time admitting separable (Hamilton-Jacobi and Klein-Gordon) equations of motion. When separability is implemented a priori, it determines certain form of the metric functions which are the functions of radial and angle coordinates. Then the Einstein-Maxwell equations for electro-vacuum space-time readily admit the most general solution which turns out to be the Kerr-NUT solution [4] establishing its uniqueness in a straightforward and direct manner. When the asymptotic flatness is imposed, the NUT parameter vanishes yielding the unique Kerr family. The Kerr family is thus included in the more general Kerr-NUT family which is the most general family for a metric admitting separable equations of motion. It would thus imply separability of the equations of motion for the Kerr family and it is indeed, as is well-known, so [1].

The most remarkable feature of this method of obtaining the most general solution is that it exposes the duality transformation which keeps the metric invariant. The duality here means exchange of the mass and NUT parameters on one hand and the radial and angular coordinates on the other [5,6]. Else the Kerr-NUT solution has been known for long [4], but this invariance has thus far remained unnoticed. Like mass is the measure of gravitational electric charge, NUT parameter is supposed to be the measure of magnetic charge [7]. The Kerr-NUT solution is therefore a truly gravitational dyon solution [6] and it represents gravitational field of a rotating body having both the gravitational

*At present: Harvard-Smithsonian Center for Astrophysics, 60 Garden Street, Cambridge, MA 02138, USA; bmukhopa@cfa.harvard.edu

electric (mass) and magnetic (NUT) charges. By the duality transformation, one can obtain the space-time dual to the Kerr solution.[1] There exists duality between the field of a rotating electric charge (M) and rotating magnetic charge (NUT parameter, l) [9] and vice-versa. Though there exists pure NUT solution [2] without the rotation parameter a, but for the duality transformation its presence is essential. That is, the duality between gravitational electric and magnetic charges could be exhibited only when the body is rotating.

The Kerr family has been studied extensively for motion of test particles as well as for the scalar, spinor, vector and tensor perturbations of the metric. In this paper, we would like to study the scalar and spinor perturbations, i.e. the Klein-Gordon and Dirac equations in the Kerr-NUT geometry. As we said earlier that by a simple duality transformation one can switch over from the Kerr solution to the dual Kerr (where $M = 0$). From the properties of the Kerr metric, it is possible to derive the corresponding properties of the dual Kerr metric. For instance, the scalar and spinor perturbation equations of the Kerr geometry can be translated to the corresponding equations for the dual geometry by the duality transformation which takes the Kerr metric to the dual Kerr metric. However, the duality works only at the equation level but not at the solution level; viz the solution of the scalar equation in the Kerr case can not be taken over to the solution of the corresponding equation in the dual case by any such simple transformations. This happens because the duality involves mass and NUT parameters and their presence and absence in the equation changes the nature of solution. In the Kerr metric there is mass parameter but no NUT parameter. Under the duality transformation, mass goes to NUT parameter and so the dual metric has NUT parameter but no mass. Hence the solution which is obtained with mass parameter present will have different character and would not go over to the one obtained with mass zero and NUT non-zero. In the present case, this has become more non-trivial due to the particular selection of variable transformation which reduces the equations into the form of wave equations whose solution is known.

The duality would have been very interesting, had it worked at the solution level as well. That unfortunately does not happen here trivially. Considering the Kerr solution as the field of rotating gravitational electric charge (M) and its dual as the field of rotating gravitational magnetic charge (l - the NUT parameter). Then it should be of interest to study the scalar and spinor perturbations of these two fields and compare their behaviour. This is exactly what we wish to do. We should however note that the dual solution is indeed an exact solution of the Einstein vacuum equation which is asymptotically non flat and its asymptotic flat limit is flat spacetime (i.e. if we impose the condition of asymptotic flatness, it reduces to flat spacetime). We shall probe this space-time with the scalar and spinor fields and compare their motion with the corresponding motion in the Kerr geometry. Our main aim here is to study the perturbations first in the general Kerr-NUT space-time and then specialize to the Kerr and the dual Kerr cases by employing the duality transformation. For the duality to work it is required that $a \neq 0$. Hence we cannot go to $a = 0$ limit of the pure NUT solution. As we are not able to establish any duality relation between the solutions in the Kerr and dual Kerr cases, we will compare the solutions graphically.

The paper is organized as follows. In §II, we shall recall the Kerr-NUT metric and its invariance under the duality

[1] It is different from the electrogravity dual of the Kerr solution [8].

transformation. Next two sections III and IV would respectively be devoted to the Klein-Gordon and Dirac equations and their transformation under the duality. In §III, we will also present the numerical solution of scalar perturbation equation. Then in §V, we shall present and discuss the various numerical solutions of the Dirac spinors which would be followed by discussion of horizon and singularity in §VI, and we end with a discussion of the main results.

II. THE KERR-NUT METRIC AND THE DUALITY

Here we study the interaction of particles of spin zero and spin half with the Kerr-NUT black hole. We are familiar with the Klein-Gordan and Dirac equations in flat space by which one can investigate the behaviour of spin zero and spin half particles. In the curved space-time the form of these equations are modified. The Dirac equation was written in the Kerr geometry by Teukolsky [10] and was separated by Chandrasekhar [11] into the radial and angular parts (for a comprehensive discussion, see [1]). Recently, there has been a fresh investigation of the radial Dirac equation in the Schwarzschild, Reissner-Nordström and Kerr geometries [12–14].

In the linearized test field approximation, scalar, vector and tensor perturbations of the Kerr geometry has been studied by several authors (e.g. [1,10]). The master equations [10] governing these linear perturbations for integral spin (e.g., gravitational and electromagnetic) fields were solved numerically by Press & Teukolsky [15] and by Teukolsky & Press [16]. Particularly interesting is the fact that whereas gravitational and electromagnetic reflected wave from the black hole was found to be amplified for certain range of incoming frequencies, however Chandrasekhar [1] predicted that no such amplification should take place for the Dirac waves because of the very nature of the potential experienced by the incoming fields.

The space-time metric for the Kerr-NUT geometry [5] is given by

$$ds^2 = -\frac{U^2}{\rho^2}\left(dt - Pd\phi\right)^2 + \frac{sin^2\theta}{\rho^2}\left[(F+l^2)d\phi - adt\right]^2 + \frac{\rho^2}{U^2}dr^2 + \rho^2 d\theta^2, \tag{1}$$

where,

$$F = r^2 + a^2, U^2 = r^2 - 2Mr + a^2 + Q_*^2 - l^2, P = asin^2\theta - 2lcos\theta, \rho^2 = r^2 + \lambda^2, \lambda = l + acos\theta. \tag{2}$$

Here, l is the NUT parameter, a and Q_* are rotation and electric charge parameters of the black hole. The most remarkable property of this metric is that it is invariant under the duality transformation, $M \leftrightarrow il, r \leftrightarrow i\lambda$ [5,6]. That is, interchange of the gravitational electric (M) and magnetic (l) charge also requires the corresponding interchange of the radial and angle coordinates. For the former, radial is the responding coordinate, while for the latter, it is the angle coordinate. Further the transformation, $M \to il, r \leftrightarrow i\lambda$ will take the Kerr solution to the dual Kerr solution, and similarly vice-versa.

Now following the Newman-Penrose formalism, we introduce null tetrads $(\vec{l}, \vec{n}, \vec{m}, \vec{\bar{m}})$ to satisfy orthogonality relations, $\vec{l}.\vec{n} = 1$, $\vec{m}.\vec{\bar{m}} = -1$ and $\vec{l}.\vec{m} = \vec{n}.\vec{m} = \vec{l}.\vec{\bar{m}} = \vec{n}.\vec{\bar{m}} = 0$. Thus we write the basis vectors of null tetrad in terms of elements of the Kerr-NUT geometry as

$$\begin{aligned} l_\mu &= \frac{1}{U^2}(U^2, -\rho^2, 0, -U^2P), \qquad n_\mu = \frac{1}{2\rho^2}(U^2, \rho^2, 0, -U^2P), \\ m_\mu &= \frac{1}{\bar{\rho}\sqrt{2}}(iasin\theta, 0, -\rho^2, -i(F+l^2)sin\theta), \qquad \bar{m}_\mu = \frac{1}{\bar{\rho}^*\sqrt{2}}(-iasin\theta, 0, -\rho^2, i(F+l^2)sin\theta) \end{aligned} \tag{3}$$

and

$$l^\mu = \frac{1}{U^2}(F+l^2, U^2, 0, a), \qquad n^\mu = \frac{1}{2\rho^2}(F+l^2, -U^2, 0, a),$$
$$m^\mu = \frac{1}{\bar{\rho}\sqrt{2}}(iPcosec\theta, 0, 1, icosec\theta), \qquad \bar{m}^\mu = \frac{1}{\bar{\rho}^*\sqrt{2}}(-iPcosec\theta, 0, 1, -icosec\theta), \tag{4}$$

where $\bar{\rho} = r + i\lambda$ and $\bar{\rho}^* = r - i\lambda$.

In the next two sections, we study perturbations to the Kerr-NUT (including the Kerr as well as the dual Kerr) space-time with the Klein-Gordan and Dirac equations and the corresponding propagation of scalar and spinor waves respectively. So the perturbation can be expressed as a superposition of stationary waves with different modes given as $e^{i(\sigma t + m\phi)}$, where σ is the frequency of the waves and m is the azimuthal quantum number.

III. THE KLEIN-GORDAN EQUATION

The general equation of scalar field (wave) in curved space-time can be written as

$$\frac{1}{\sqrt{-g}}\partial_\mu\left(\sqrt{-g}g^{\mu\nu}\partial_\nu\Psi\right) - m_p^2\Psi = 0 \tag{5}$$

where m_p is the mass of the scalar field. Now substituting $\Psi = e^{i(\sigma t+m\phi)}\Phi$ in (5) we get

$$\left(\frac{(F+l^2)^2}{U^2} - \frac{P^2}{sin^2\theta}\right)\sigma^2\Phi + \frac{\partial}{\partial r}(U^2\Phi_{,r}) + \frac{a(2l^2 - Q_*^2 + 2Mr) + 2lU^2 cot\theta cosec\theta}{U^2}(2\sigma m)\Phi$$
$$+ \left(\frac{a^2}{U^2} - \frac{1}{sin^2\theta}\right)m^2\Phi + \frac{1}{sin\theta}\frac{\partial}{\partial\theta}(\Phi_{,\theta}sin\theta) + m_p^2\rho^2\Phi = 0. \tag{6}$$

Further choosing $\Phi = R_0(r)S_0(\theta)$ and separating the radial and angular parts of (6) we write

$$\left[\frac{\partial^2}{\partial\theta^2} + cot\theta\frac{\partial}{\partial\theta} - \frac{P^2\sigma^2}{sin^2\theta} + 4l\sigma m cot\theta cosec\theta + \lambda_1^2 + m_p^2(l + acos\theta)^2 - \frac{m^2}{sin^2\theta}\right]S_0 = 0, \tag{7}$$

$$\left[U^2\frac{\partial^2}{\partial r^2} + 2(r-M)\frac{\partial}{\partial r} + \frac{\sigma^2}{U^2}(F+l^2)^2 + r^2m_p^2 + \frac{a^2m^2}{U^2} + \frac{2a\sigma m}{U^2}(2l^2 - Q_*^2 + 2Mr) - \lambda_1^2\right]R_0 = 0, \tag{8}$$

where λ_1 is the separation constant.

It is interesting to note that, following [5], if we perform the duality transformation $M \leftrightarrow il$, $r \leftrightarrow i\lambda$ and $R_0 \leftrightarrow S_0$, and with suitable redefinition of a, Eqns. (7) and (8) remain invariant. Further, under the duality transformation, $M \to il$, $r \leftrightarrow i\lambda$ and $R_0 \leftrightarrow S_0$, Eqns. (7) and (8) for the Kerr solution (with $l = 0$) will go over to that of the dual Kerr solution (with $M = 0$). Similarly, the reverse duality transformation, $l \to -iM$, $r \leftrightarrow i\lambda$ and $R_0 \leftrightarrow S_0$, will bring the equations back to the Kerr geometry.

Let us choose the transformation of independent variables r and θ as

$$y = \frac{1}{2}log\left(\frac{1-cos\theta}{1+cos\theta}\right), \qquad z = \frac{r^3}{3} - (r_+ + r_-)\frac{r^2}{2} + r_+r_-r, \tag{9}$$

where $r_\pm = M \pm \sqrt{M^2 + l^2 - a^2 - Q_*^2}$ and further

$$Z = U^2R_0. \tag{10}$$

Thus from (7), (8), (9) and (10) we get

$$\frac{d^2S_0}{dy^2} + V_y S_0 = 0, \tag{11}$$

$$\frac{d^2Z}{dz^2} + V_z Z = 0, \tag{12}$$

where

$$V_y = \lambda_1^2 sin^2\theta - P^2\sigma^2 + 4l\sigma m cos\theta + m_p^2 sin^2\theta(l + acos\theta)^2 - m^2, \tag{13}$$

$$V_z = \frac{1}{U^6}\left(\sigma^2(F + l^2)^2 + a^2m^2 + 2a\sigma m(2l^2 - Q_*^2 + 2Mr) + r^2U^2m_p^2 - \lambda_1^2U^2 + \frac{4(r-M)^2}{U^2} - 2\right). \tag{14}$$

Here V_y and V_z are the effective gravitational potentials for angular and radial motion respectively of the scalar field. At $\theta = 0$ and π and the corresponding $y = -\infty$ and ∞, V_y reduces to $-(2l\sigma - m)^2$ and $-(2l\sigma + m)^2$ respectively. From (13) it is clear that V_y scales with l and a. Keeping the other parameters unchanged if l and/or a increases so does the potential. In the case of the radial potential, V_z, it falls off at large r but it diverges at the horizon [see Eqn. (14)]. Physically it means that the perturbation at large distance should not affect the space-time near the black hole. With the perturbation propagating towards the horizon, its effect becomes important. Here, note that in the natural units ($G = c = h = 1$), all the parameters are dimensionless.

Equations (11) and (12) are the simple one-dimensional wave equations which we solve numerically and depict in Figs. 1 and 2 for the Kerr-NUT, Kerr and dual Kerr space-times with a certain choice of parameters. In principle, one should first solve the angular equation with the eigenvalue, λ_1. Then inserting that value of λ_1 into the radial equation, one should solve the radial equation. However, at the first instance we would like to get a qualitative feeling of the solution and hence we have set here $\lambda_1 = 1$ throughout. This is a deficiency of the solutions presented here which are not complete in this sense. However, they do provide some useful qualitative insight. In future we plan to evaluate λ_1 and get the complete solution. Here our main aim is just to give an indication of form of the possible solution. We use the Runge-Kutta method with the natural boundary conditions at infinity. We know that at infinity the potential barrier is either zero or constant. Therefore the wave form should be sinusoidal which defines the boundary condition at infinity. For the angular solution, first note that V_y is independent of the mass M and hence it is the same for the Kerr-NUT and the dual Kerr space-times. From the Figs. 1 and 2, the variance of solutions as a function of the rest mass of the incoming scalar as well as the space-time parameters, a, l and M, is very clear. Figure 1 shows that the amplitude of the solution is significantly high for the Kerr case. This is because the net gravitational effect is stronger for the Kerr case than the Kerr-NUT. It should be noted that the NUT and rotation parameters tend to oppose each other. Also the solution shows the existence of singularity in the space-time at $\theta \to 0$. On the other hand, Fig. 2 indicates an extension of the inner space-time region down to $r = 0$ for the dual Kerr and thus the wavelength of scalar waves would therefore be wider than that for the Kerr and Kerr-NUT metrics. For the radial mode, larger is the wavelength for less massive perturbation.

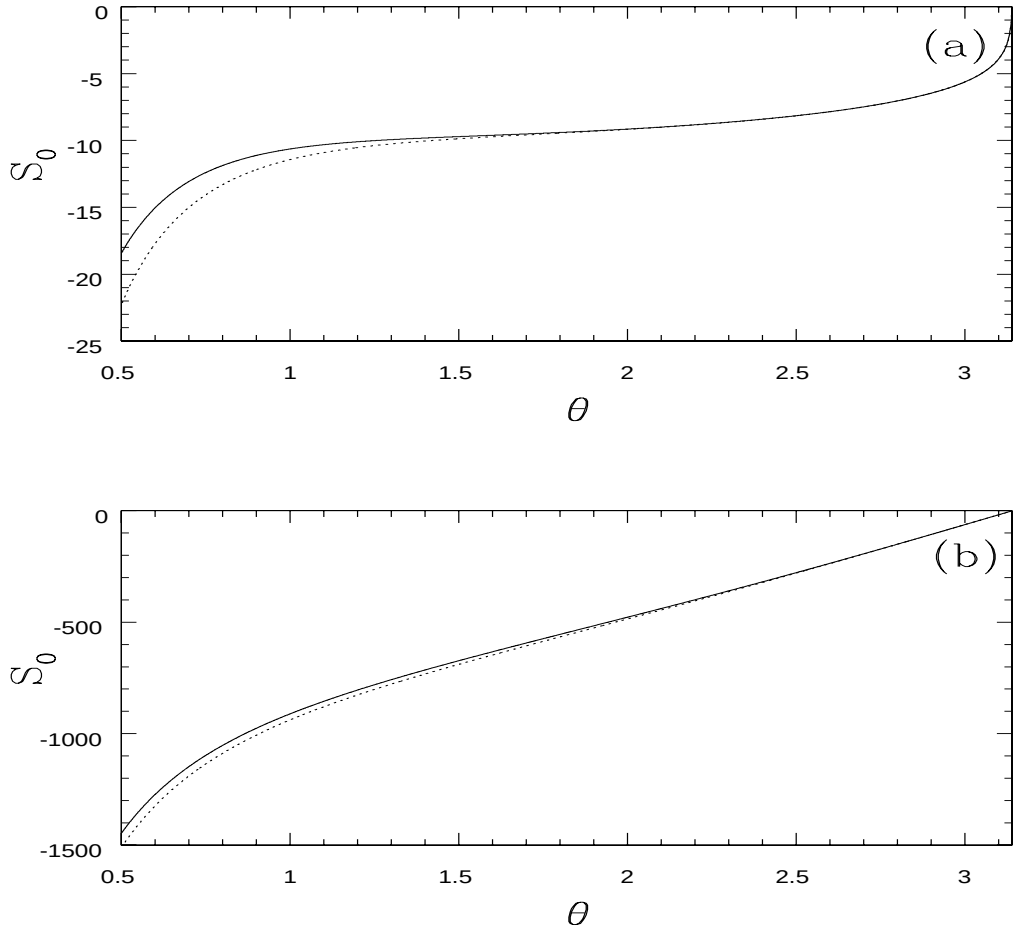

FIG. 1. Angular Klein-Gordan solution with $\sigma = 0.4$, $M = 1$ for (a) Kerr-NUT, $a = 0.998$, $l = 0.99$, (b) Kerr, $a = 0.998$. Solid and dotted curves indicate the cases, $m_p = 0.4, 0.1$ respectively.

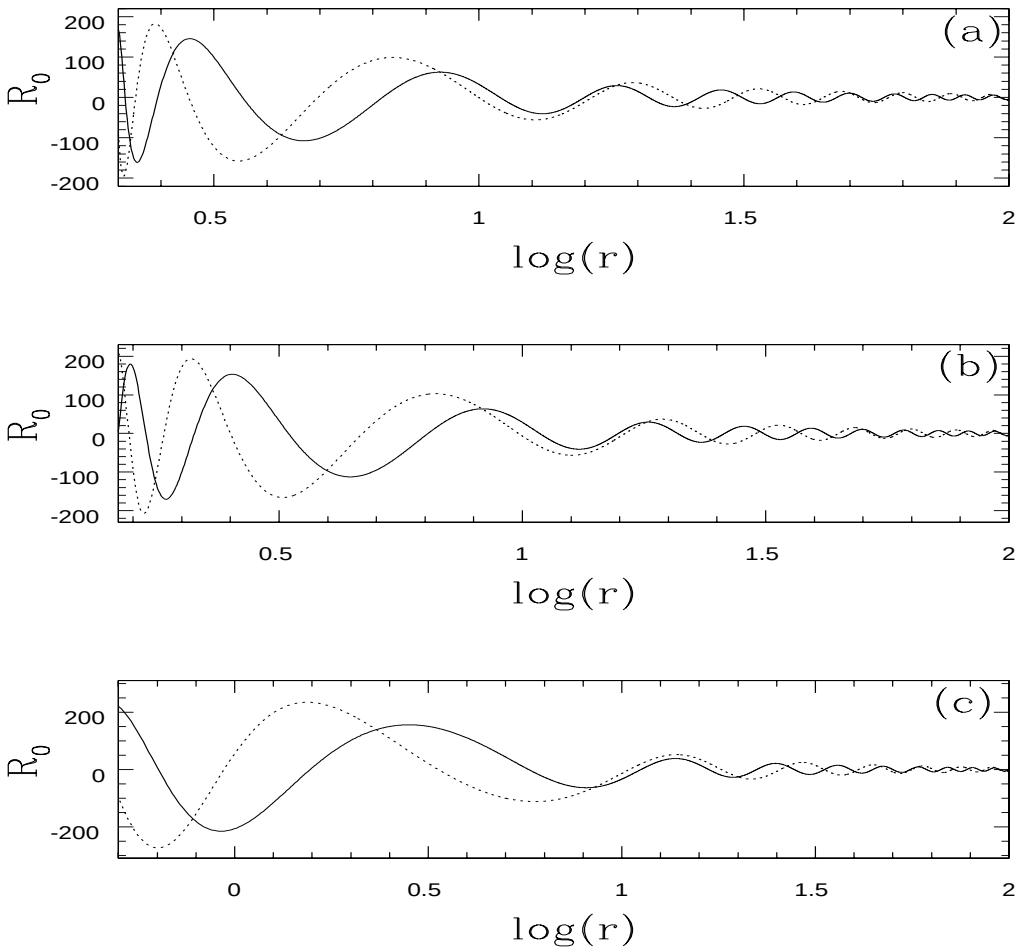

FIG. 2. Radial Klein-Gordan solution with $\sigma = 0.4$, for (a) Kerr-NUT, $a = 0.998$, $l = 0.99$, (b) Kerr, $a = 0.998$, (c) dual Kerr, $a = l = 0.998$. Solid and dotted curves indicate the cases, $m_p = 0.4, 0.1$ respectively. $M = 1$ for (a) and (b).

Note that the Klein-Gordon equation remains invariant under the duality transformation and the equation for the Kerr geometry can be transformed to that for the dual Kerr geometry and vice versa, but as is mentioned in §1 there is no easy way to exploit *explicitly* this duality for the solutions. One of the reason behind this is due to the certain choice of the independent variables to cast the equation in the familiar simple form which facilitates the analysis of motion through the behaviour of potential. The angular potential, V_y, depends upon the NUT parameter, l, and is free of the mass of the black hole. The Kerr solution has only kinematic part coming from the rotation parameter, a. While the radial potential, V_z, depends upon both M and l. We can go to the corresponding potential and solutions for the Kerr and the dual Kerr space-times by setting $l = 0$ and $M = 0$ respectively in the Eqns. (13) and (14).

IV. THE DIRAC EQUATION

Following [14], derivative of spinor P^A can be written as

$$D_\mu P^A = \partial_\mu P^A + iqA_\mu P^A + \Gamma^A_{\mu\nu} P^\nu, \tag{15}$$

where A_μ and $\Gamma^A_{\mu\nu}$ are electromagnetic and gravitational gauge fields respectively. Thus, the Dirac equation in the Newman-Penrose formalism can be written as

$$\sigma^\mu_{AB'} D_\mu P^A + i\mu_p \bar{Q}^{C'} \epsilon_{C'B'} = 0, \tag{16}$$

$$\sigma^\mu_{AB'} D_\mu Q^A + i\mu_p \bar{P}^{C'} \epsilon_{C'B'} = 0. \tag{17}$$

For a vector X_i, $\sigma^i_{AB'} X_i = X_{AB'}; A, B = 0, 1$; and $2^{\frac{1}{2}}\mu_p$ is the mass of the Dirac particle. In terms of this new basis of the Newman-Penrose formalism, the Pauli matrices can be written as

$$\sigma^\mu_{AB'} = \frac{1}{\sqrt{2}} \begin{pmatrix} l^\mu & m^\mu \\ \bar{m}^\mu & n^\mu \end{pmatrix}. \tag{18}$$

Following [1] and writing

$$P^0 = F_1, P^1 = F_2, \bar{Q}^{1'} = G_1, \bar{Q}^0 = -G_2$$

we get

$$l^\mu(\partial_\mu + iqA_\mu)F_1 + \bar{m}^\mu(\partial_\mu + iqA_\mu)F_2 + (\epsilon - \tilde{\rho})F_1 + (\pi - \alpha)F_2 = i\mu_p G_1, \tag{19}$$

$$m^\mu(\partial_\mu + iqA_\mu)F_1 + n^\mu(\partial_\mu + iqA_\mu)F_2 + (\mu - \gamma)F_2 + (\beta - \tau)F_1 = i\mu_p G_2, \tag{20}$$

$$l^\mu(\partial_\mu + iqA_\mu)G_2 - m^\mu(\partial_\mu + iqA_\mu)G_1 + (\epsilon^* - \tilde{\rho}^*)G_2 - (\pi^* - \alpha^*)G_1 = i\mu_p F_2, \tag{21}$$

$$n^\mu(\partial_\mu + iqA_\mu)G_1 - \bar{m}^\mu(\partial_\mu + iqA_\mu)G_2 + (\mu^* - \gamma^*)G_1 - (\beta^* - \tau^*)G_2 = i\mu_p F_1. \tag{22}$$

These are the Dirac equations in the curved space-time.

We define the spinor fields as follows:

$$f_1 = e^{i(\sigma t + m\phi)}\bar{\rho}^* F_1, \quad f_2 = e^{i(\sigma t + m\phi)} F_2, \quad g_1 = e^{i(\sigma t + m\phi)} G_1, \quad g_2 = e^{i(\sigma t + m\phi)}\bar{\rho} G_2 \tag{23}$$

and the electromagnetic vector potential, $A_\mu = (A_t, 0, 0, A_\phi)$. For the Kerr-NUT metric, it can be expressed as

$$A_t = -\frac{rQ_*}{\rho^2}, \qquad A_\phi = \frac{rQ_* P}{\rho^2}. \tag{24}$$

We also list the spin coefficients in terms of the Kerr-NUT metric as

$$\begin{aligned} &\tilde{\rho} = -\frac{1}{\bar{\rho}^*}, \quad \beta = \frac{cot\theta}{2\sqrt{2}\bar{\rho}}, \quad \pi = \frac{iasin\theta}{\sqrt{2}(\bar{\rho}^*)^2}, \quad \epsilon = 0, \\ &\tau = -\frac{iasin\theta}{\rho^2\sqrt{2}}, \quad \mu = -\frac{U^2}{2\rho^2\bar{\rho}^*}, \quad \gamma = \mu + \frac{r - M}{2\rho^2}, \quad \alpha = \pi - \beta^*. \end{aligned} \tag{25}$$

Now by substituting Eqns. (23-25) into Eqns. (19-22), we reduce the Dirac equation to

$$\mathcal{D}_0 f_1 + 2^{-\frac{1}{2}}\mathcal{L}_{\frac{1}{2}} f_2 = [i\mu_p r + \mu_p(l + acos\theta)]g_1 \tag{26}$$

$$U^2\mathcal{D}^\dagger_{\frac{1}{2}} f_2 - 2^{\frac{1}{2}}\mathcal{L}^\dagger_{\frac{1}{2}} f_1 = -2[i\mu_p r + \mu_p(l + acos\theta)]g_2 \tag{27}$$

$$\mathcal{D}_0 g_2 - 2^{-\frac{1}{2}}\mathcal{L}^\dagger_{\frac{1}{2}} g_1 = [i\mu_p r - \mu_p(l + acos\theta)]f_2 \tag{28}$$

$$U^2\mathcal{D}^\dagger_{\frac{1}{2}} g_1 + 2^{\frac{1}{2}}\mathcal{L}_{\frac{1}{2}} g_2 = -2[i\mu_p r - \mu_p(l + acos\theta)]f_1 \tag{29}$$

where,

$$\begin{aligned}\mathcal{D}_n &= \frac{d}{dr} + \frac{i}{U^2}(\sigma(F + l^2) + am + qQ_* r) + 2n\frac{r - M}{U^2},\\ \mathcal{D}^\dagger_n &= \frac{d}{dr} - \frac{i}{U^2}(\sigma(F + l^2) + am + qQ_* r) + 2n\frac{r - M}{U^2}\end{aligned} \tag{30}$$

and

$$\begin{aligned}\mathcal{L}_n &= \frac{d}{d\theta} + (\sigma P + m)cosec\theta + ncot\theta,\\ \mathcal{L}^\dagger_n &= \frac{d}{d\theta} - (\sigma P + m)cosec\theta + ncot\theta.\end{aligned} \tag{31}$$

Further writing $f_1(r,\theta) = R_{-\frac{1}{2}}(r)S_{-\frac{1}{2}}(\theta)$, $f_2(r,\theta) = R_{\frac{1}{2}}(r)S_{\frac{1}{2}}(\theta)$, $g_1(r,\theta) = R_{\frac{1}{2}}(r)S_{-\frac{1}{2}}(\theta)$, $g_2(r,\theta) = R_{-\frac{1}{2}}(r)S_{+\frac{1}{2}}(\theta)$, we can separate Eqns (26)-(29) into angular and radial parts as

$$\mathcal{L}_{1/2}S_{1/2} = -(\lambda_2 - m_p(l + acos\theta))S_{-1/2}, \qquad \mathcal{L}^\dagger_{1/2}S_{-1/2} = (\lambda_2 + m_p(l + acos\theta))S_{1/2}, \tag{32}$$

$$U\mathcal{D}_0 R_{-1/2} = (\lambda_2 + im_p r)UR_{1/2}, \qquad U\mathcal{D}^\dagger_0 UR_{1/2} = (\lambda_2 - im_p r)R_{-1/2}. \tag{33}$$

Here, m_p is the normalized rest mass of the incoming particle and λ_2 is the separation constant. Unlike the case of the scalar perturbation, the invariance of the spinor perturbation equations under the duality transformation is non trivial, as the up and down spinor components couple with each other. However, if we choose the duality relations between spinor components as $iS_{1/2} \leftrightarrow U^{-1/2}R_{-1/2}$ and $S_{-1/2} \leftrightarrow U^{1/2}R_{1/2}$, Eqns. (32-33) do remain invariant when $M \leftrightarrow il$, $r \leftrightarrow i\lambda$. As before, then we can switch over the Dirac equation in the Kerr space-time to that in the dual Kerr space-time and vice versa by the duality transformation. Further the interesting point to note is that under the duality transformation, the up-spinor transforms to the down and vice versa, with the multiplication/division of U. Next we study the separated angular and radial equations.

IV.A. Angular equations

If we decouple the equations in (32) for $S_{-\frac{1}{2}}$, we get

$$\mathcal{L}_{\frac{1}{2}}\mathcal{L}^\dagger_{\frac{1}{2}} S_{-\frac{1}{2}} + \frac{m_p asin\theta}{\lambda + m_p(l + acos\theta)}\mathcal{L}^\dagger_{\frac{1}{2}} S_{-\frac{1}{2}} + (\lambda_2^2 - m_p^2(l + acos\theta)^2)S_{-\frac{1}{2}} = 0. \tag{34}$$

Similarly one can decouple the equations in (32) for $S_{\frac{1}{2}}$. Let us choose

$$u_\mp = \left(\lambda_2 \pm m_p l \pm \frac{m_p a}{2}\right) log(1 - cos\theta) - \left(\lambda_2 \pm m_p l \mp \frac{m_p a}{2}\right) log(1 + cos\theta). \tag{35}$$

Thus the decoupled equations for $S_{-\frac{1}{2}}$ [i.e. Eqn. (34)], and for $S_{\frac{1}{2}}$ [not given here], can be reduced to

$$\frac{d^2 S_{\mp\frac{1}{2}}}{du_{\mp}^2} + W_{\mp} S_{\mp\frac{1}{2}} = 0 \tag{36}$$

where

$$W_{\mp} = \frac{sin^2\theta}{(\lambda_2 \pm m_p(l + acos\theta))^2}\left[\pm(\sigma P + m)cot\theta cosec\theta + \sigma cosec\theta(2asin\theta cos\theta + 2lsin\theta) - \frac{cosec^2\theta}{2} + \frac{cot^2\theta}{4}\right.$$
$$\left. - (\sigma P + m)^2 cosec^2\theta + \lambda_2^2 - m_p^2(l + acos\theta)^2 \pm \frac{m_p a sin\theta}{\lambda_2 \pm m_p(l + acos\theta)}\left(\frac{cot\theta}{2} \mp (\sigma P + m)cosec\theta\right)\right]. \tag{37}$$

Eqn. (36) is a simple one dimensional wave equation. Here again the angular potential depends upon l and is free off M.

The above gravitational potentials are related to the physical parameters and variable in a rather complicated manner compared to the case of scalar perturbation. For both $\theta \to 0$ and π, angular potential barriers reduce to zero ($W_{\pm} \to 0$). We can study the potential barriers felt by the incoming spinors with different masses and frequencies. In principle one can choose any mass and frequency of the field but to bring a significant interaction with the black hole we choose the mass and frequency in such a manner that the Compton wavelength of the incoming fields becomes same order as the radius of the outer horizon to the black hole. Also the frequency of the perturbation should be same order as the inverse of the light crossing time to the radius of the black hole. Thus we choose

$$\sigma \sim m_p \sim r_+^{-1}. \tag{38}$$

Figures 3 and 4 indicate the behaviour of potentials felt by the spinors in the angular direction in the transformed coordinate system. For a particular σ, as m_p decreases the coupling strength between the spinor and space-time curvature reduces then the peak of the barrier goes down. Similarly for the same m_p if σ reduces the peak goes down. The interesting feature that emerges out is that the height of the barrier is quite sensitive to the spin orientation (up/down) of the incoming spinor field. This is in accordance with the expectation that a spinning black hole (with a particular spin orientation) can distinguish the up and down spin of the perturbation separately. Further a spinor feels higher potential barrier when it is aligned with the black hole. We also note the mirror inversion symmetry between W_+ and W_-.

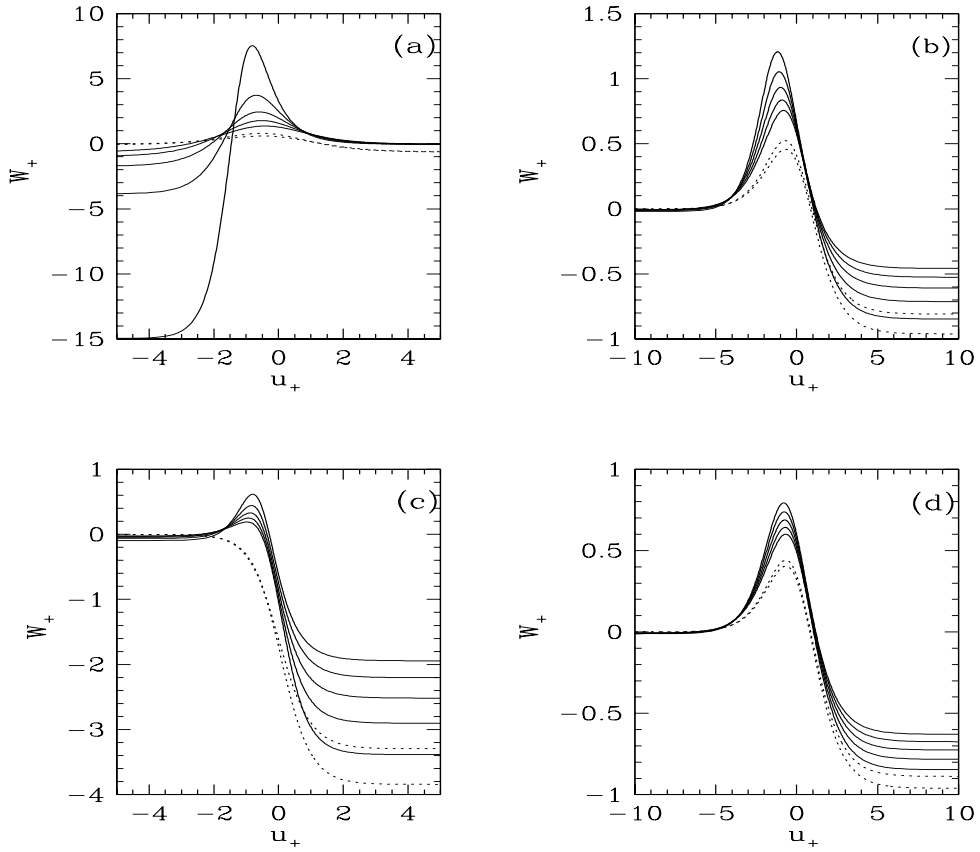

FIG. 3. Variation of W_+ as a function of u_+, $M = 1$ when (a) $a = 0.998$, $l = 0.99$, (b) $a = 0.998$, $l = 0.1$, (c) $a = l = 0.5$, (d) $a = 0.5$, $l = 0.1$. Solid curves indicate the cases, $\sigma = 0.4$; $m_p = 0.4, 0.3, 0.2, 0.1, 0$ from top to bottom and dotted curves indicate $\sigma = 0.1$; $m_p = 0.1, 0$ from top to bottom.

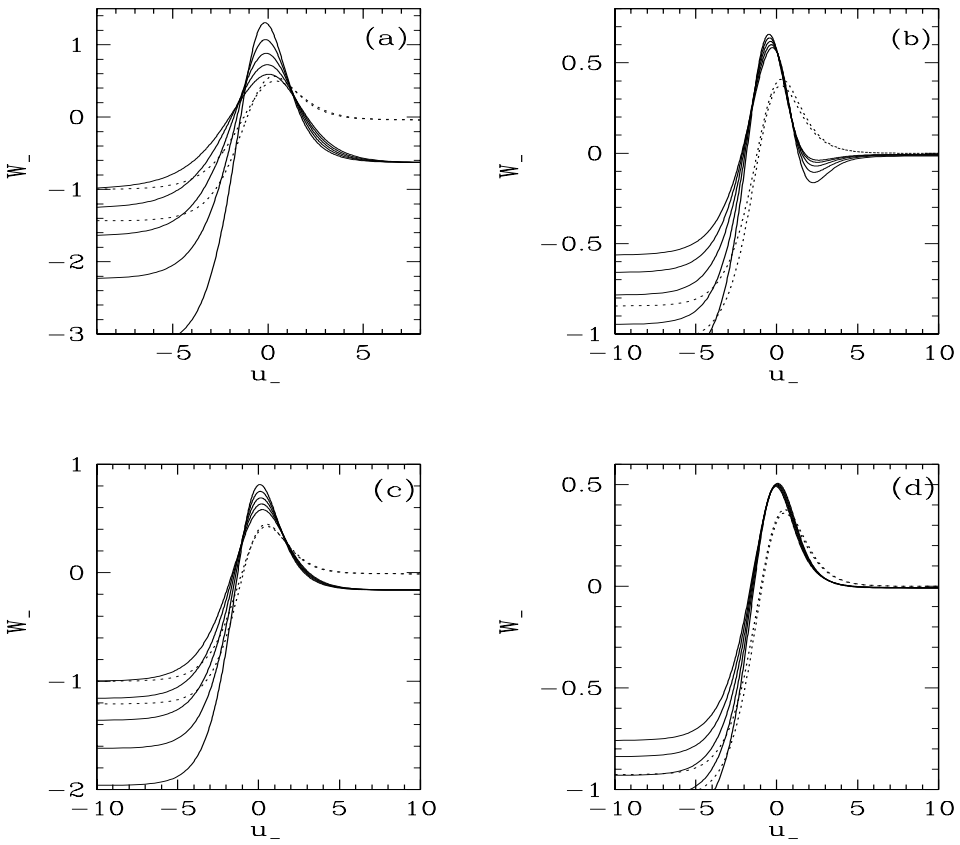

FIG. 4. Variation of W_- as a function of u_-, $M = 1$ when (a) $a = 0.998$, $l = 0.99$, (b) $a = 0.998$, $l = 0.1$, (c) $a = l = 0.5$, (d) $a = 0.5$, $l = 0.1$. Solid curves indicate the cases, $\sigma = 0.4$; $m_p = 0.4, 0.3, 0.2, 0.1, 0$ from top to bottom and dotted curves indicate $\sigma = 0.1$; $m_p = 0.1, 0$ from top to bottom.

IV.B. Radial equations

Decoupling the equations in Eqn. (33) for $R_{-\frac{1}{2}}$ we write

$$U^2\mathcal{D}^\dagger_{\frac{1}{2}}\mathcal{D}_0 R_{-\frac{1}{2}} - \frac{im_pU^2}{\lambda_2 + im_pr}\mathcal{D}_0 R_{-\frac{1}{2}} - (\lambda_2^2 + m_p^2r^2)R_{-\frac{1}{2}} = 0. \tag{39}$$

However, following the earlier works [1,13], we cast this into the form,

$$\frac{d^2Z_\pm}{d\hat{r}_*^2} + \left(\sigma^2 - V_\pm\right)Z_\pm = 0 \tag{40}$$

which is easier to attack. Here we define

$$Z_\pm = UR_{\frac{1}{2}}e^{i\Theta/2} \pm R_{-\frac{1}{2}}e^{-i\Theta/2}, \qquad \Theta = tan^{-1}\left(\frac{m_pr}{\lambda}\right), \tag{41}$$

$$\hat{r}_* = r + \frac{2Mr_+ - Q_*^2 + 2l^2 + \frac{am+qQ_*r_+}{\sigma}}{r_+ - r_-}log\left(\frac{r}{r_+} - 1\right) - \frac{2Mr_- - Q_*^2 + 2l^2 + \frac{am+qQ_*r_-}{\sigma}}{r_+ - r_-}log\left(\frac{r}{r_-} - 1\right)$$
$$+ \frac{1}{2\sigma}tan^{-1}\left(\frac{m_pr}{\lambda}\right), \tag{42}$$

$$V_{\pm} = \frac{U(\lambda_2^2 + m_p^2 r^2)^{3/2}}{[\omega^2(\lambda_2^2 + m_p^2 r^2) + \frac{\lambda_2 m_p U^2}{2\sigma}]^2}[U(\lambda_2^2 + m_p^2 r^2)^{3/2} \pm \{(r-M)(\lambda_2^2 + m_p^2 r^2) + 3m_p^2 r U^2\}]$$
$$\mp \frac{U^3(\lambda_2^2 + m_p^2 r^2)^{5/2}}{[\omega^2(\lambda_2^2 + m_p^2 r^2) + \frac{\lambda_2 m_p U^2}{2\sigma}]^3}\left[\left(2r + \frac{qQ_*}{\sigma}\right)(\lambda_2^2 + m_p^2 r^2) + 2m_p^2\omega^2 r + \frac{\lambda_2 m_p (r-M)}{\sigma}\right], \tag{43}$$

where

$$\omega^2 = r^2 + \alpha^2, \;\; \alpha^2 = a^2 + l^2 + \frac{am}{\sigma} + \frac{qQ_* r}{\sigma}. \tag{44}$$

From Eqn. (42), it is clear that for

$$\sigma = \sigma_s = -\frac{qQ_* r_+ + am}{2(Mr_+ + l^2) - Q_*^2}, \tag{45}$$

coefficient of $log\left(\frac{r}{r_+} - 1\right)$ vanishes and thus for $\sigma \leq \sigma_s$, the relation $\hat{r}_* - r$ becomes multivalued. From Eqn. (43) it is clear that the potential, $V_{\pm}$, diverges at $r = |\alpha|$. This regime where $V_{\pm}$ diverges, is well known as super-radiance. For $\sigma > \sigma_s$, $|\alpha| < r_+$, and the wave can not reach at $r = |\alpha|$ and hence there is no question of super-radiance. For $\sigma = \sigma_s$, $|\alpha| = r_+$, and the potential [Eqn. (43)] diverges exactly at the event horizon. For $\sigma > \sigma_s$, $\hat{r}_*$ runs from $-\infty$ to ∞ as r varies from r_+ to ∞; but for $\sigma \leq \sigma_s$, at both $r \to r_+$ and $r \to \infty$, $\hat{r}_* \to \infty$. The turning point of the $\hat{r}_* - r$ relation occurs at $r = |\alpha|$. Thus the analogue of ergo-sphere is defined by the region $r_+ \leq r \leq |\alpha|$. However, the spinor particles do not experience super-radiance and hence no energy can be extracted by the spinor perturbation (e.g. [1,13,18]). However the result is non null for the electromagnetic perturbation and energy is possible to extract from the black hole.

It is clear from Eqn. (43) that, like angular potential barrier, here also the gravitational potentials are related to the physical parameters and variable in a complicated manner. Close to the horizon, the potential barrier, $V_{\pm}$, reduces to zero but at a large distance $V_{\pm} \to m_p^2$. Thus from Eqn. (40), it appears that σ has to be greater than or equal to m_p, otherwise spinors can not enter into the gravitational field.

Figures 5 and 6 show the behaviour of potential barriers ($V_{\pm}$) for different choices of the frequency and mass of the spinor. Here also we choose $\sigma \sim m_p \sim r_+^{-1}$, to consider a significant interaction between the incoming spinor and the black hole. For a particular frequency, as the mass of the spinor decreases the asymptotic height of the barrier decreases.

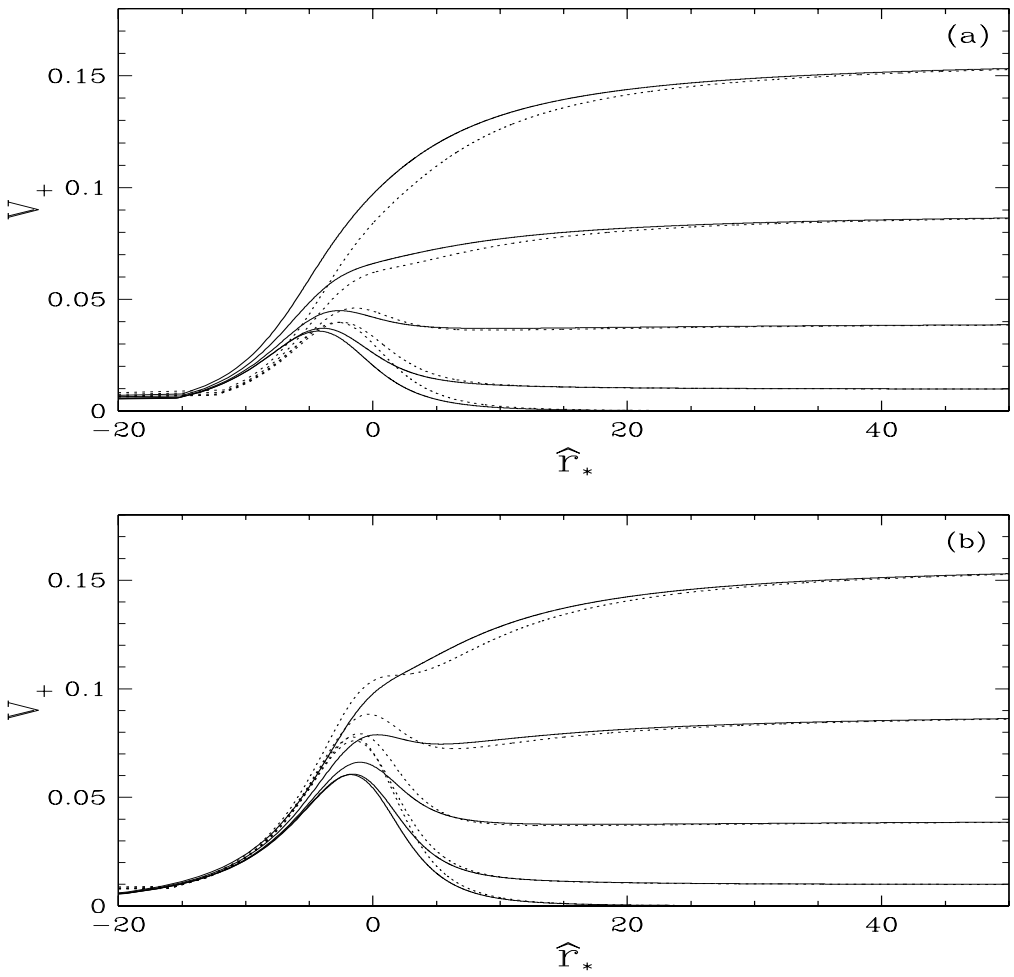

FIG. 5. Variation of V_+ as a function of $\hat{r}_*$ for $\sigma > \sigma_s$, when (a) $a = 0.998$, $l = 0.99$, (b) $a = 0.998$, $l = 0.1$. Solid curves are for $\sigma = 0.7$ and dotted curves for $\sigma = 0.4$. From the top to bottom m_p varies as $0.4, 0.3, 0.2, 0.1, 0$, and $M = 1$, $m = -1/2$, $Q_* = 0$.

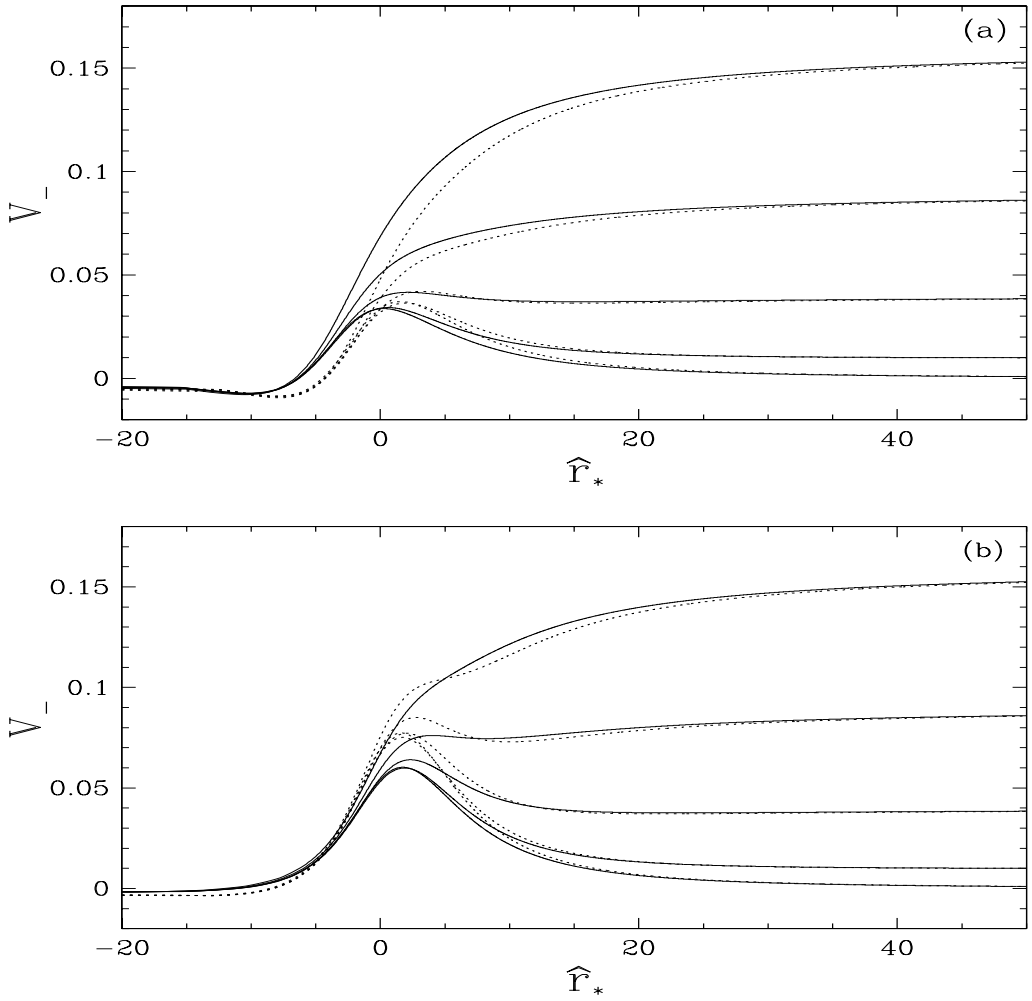

FIG. 6. Variation of V_{-} as a function of $\hat{r}_*$ for $\sigma > \sigma_s$, when (a) $a = 0.998$, $l = 0.99$, (b) $a = 0.998$, $l = 0.1$. Solid curves are for $\sigma = 0.7$ and dotted curves for $\sigma = 0.4$. From the top to bottom m_p runs through $0.4, 0.3, 0.2, 0.1, 0$, and $M = 1$, $m = -1/2$, $Q_* = 0$.

In Fig. 7, the behaviour of potentials (V_+) in super-radiance regime is shown. Clearly, at a certain r the potential diverges. For a particular σ, if m_p increases, the singular point shifts outward. The behaviour of corresponding V_{-} is similar.

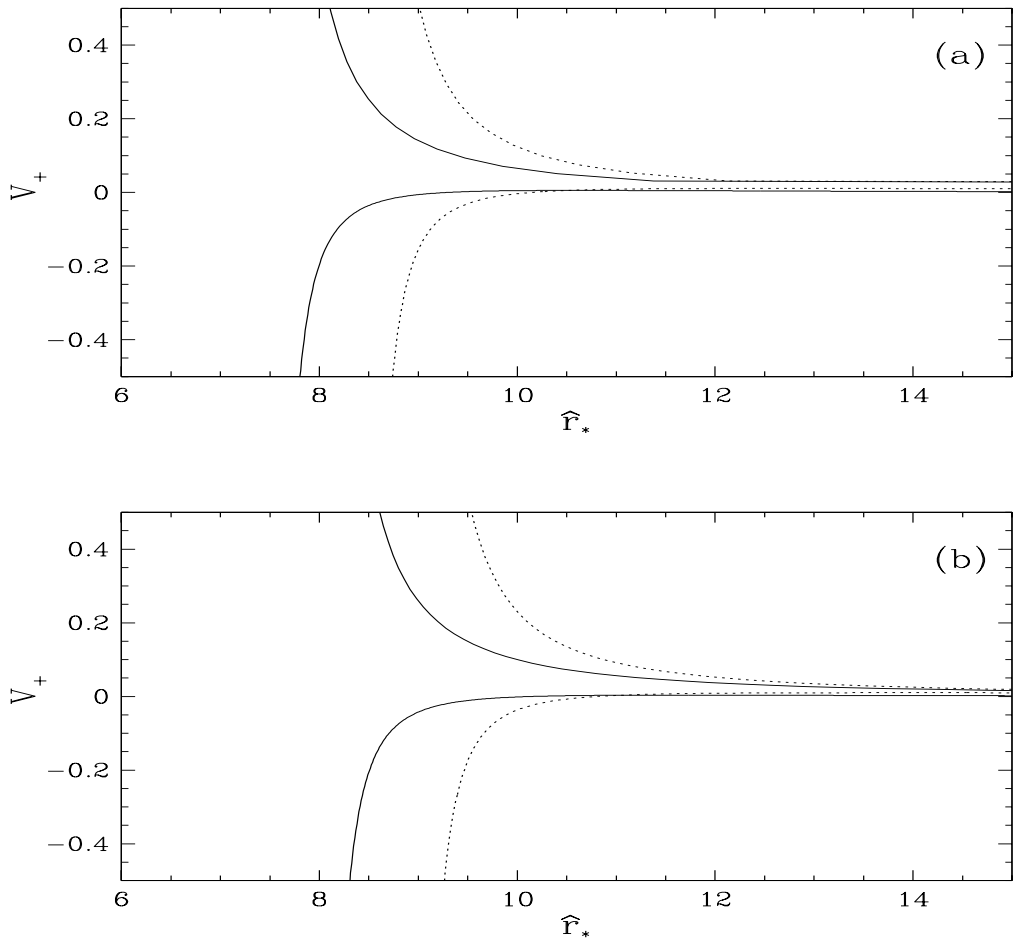

FIG. 7. Variation of V_+ as a function of $\hat{r}_*$ for $\sigma \leq \sigma_s$ ($\sigma = 0.1$), when (a) $a = 0.998$, $l = 0.5$, (b) $a = 0.998$, $l = 0.1$. Solid and dotted curves indicate $m_p = 0, 0.1$ respectively with $M = 1$, $m = -1/2$, $Q_* = 0$

IV.C. Comparison of Kerr with dual Kerr

For the dual Kerr solution $M = 0$, the corresponding $\hat{r}_*$ would read as

$$\hat{r}_* = r - \frac{\alpha^2}{r} + \frac{1}{2\sigma} tan^{-1}\left(\frac{m_p r}{\lambda}\right) \tag{46}$$

for $a = l$, and

$$\hat{r}_* = r + \frac{2l^2 + \frac{a\sigma}{m}}{\sqrt{a^2 - l^2}} tan^{-1}\frac{r}{\sqrt{a^2 - l^2}} + \frac{1}{2\sigma} tan^{-1}\left(\frac{m_p r}{\lambda}\right) \tag{47}$$

for $a > l$. The radial potential would depend upon a and l only, keeping unchanged the form of Eqn. (43).

Figures 8 and 9 show the variation of angular potential in the Kerr and dual of Kerr metrics. It is seen that the peak of the barrier (and the maximum height of it) in the dual Kerr for a particular set of σ and m_p is higher than that in the Kerr case. However $W_\pm$ in the dual Kerr is the same as for the Kerr-NUT for the angular motion because of its M independence. As before, here again W_+ is higher than W_- because of the opposite spin orientation of the perturbation, particularly in the higher frequency regime.

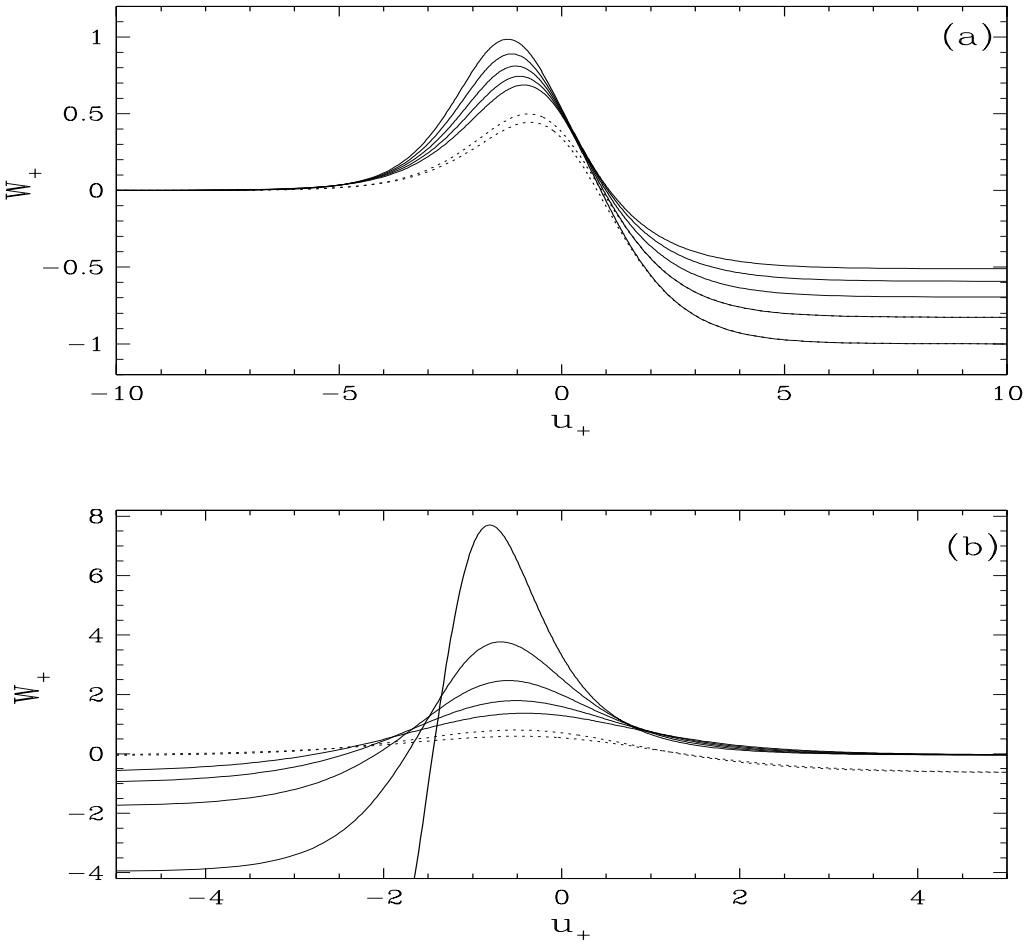

FIG. 8. Variation of W_+ for the dual Kerr ($M = 0$) case as a function of u_+ for (a) $a = 0.998$, $l = 0$, $M = 1$ (Kerr) (b) $a = l = 0.998$. From top to bottom, solid curves are for $\sigma = 0.4$; $m_p = 0.4, 0.3, 0.2, 0.1, 0$ while dotted are for $\sigma = 0.1$; $m_p = 0.1, 0$, and $m = -1/2$, $Q_* = 0$.

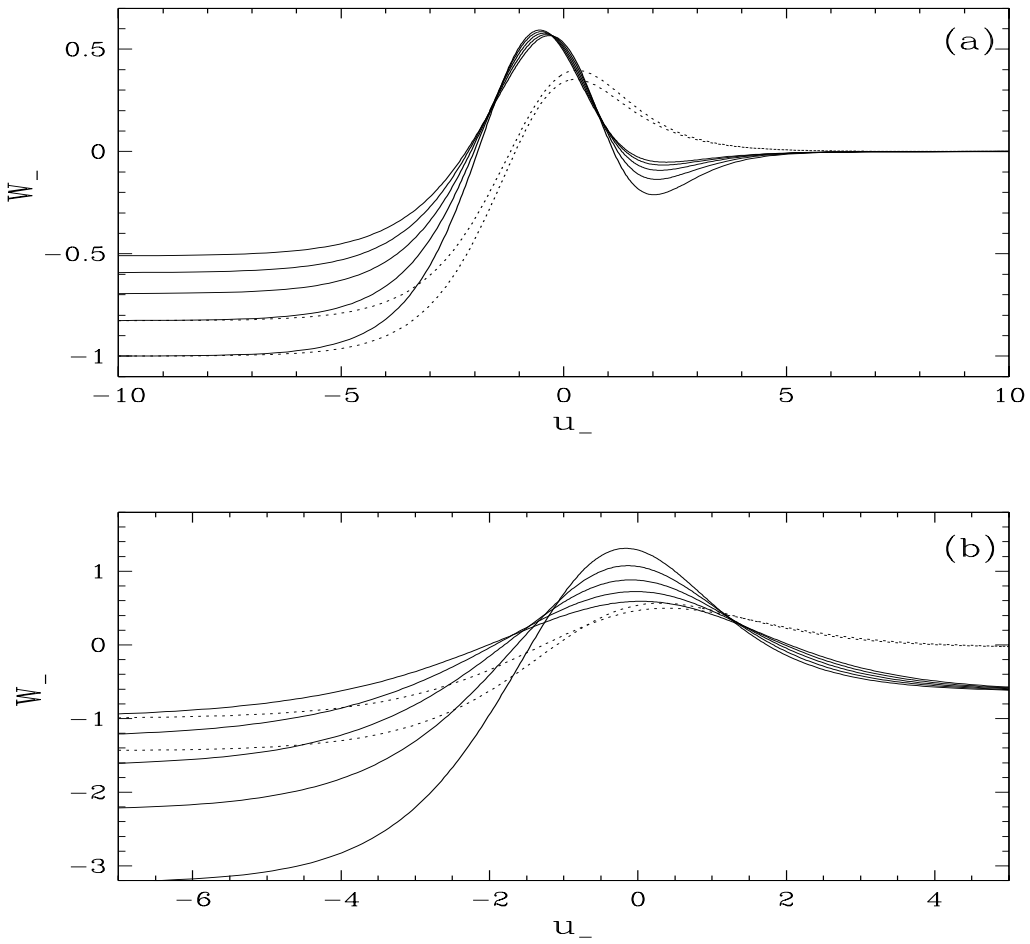

FIG. 9. Potential W_- is plotted against u_- for (a) $a = 0.998$, $l = 0$, $M = 1$ (Kerr) (b) $a = l = 0.998$, $M = 0$ (dual Kerr). From top to bottom, solid curves are for $\sigma = 0.4$; $m_p = 0.4, 0.3, 0.2, 0.1, 0$ and dotted are for $\sigma = 0.1$; $m_p = 0.1, 0$, and $m = -1/2$, $Q_* = 0$.

In Figs. 10 and 11, we compare the radial gravitational potential in the Kerr and dual Kerr cases. It is again seen that the peak of the barrier (and the maximum height of it) in the dual Kerr for a particular set of σ and m_p is higher than that in the Kerr. In the dual Kerr, for a particular m_p, if σ decreases, the peak of the barrier distinctly increases.

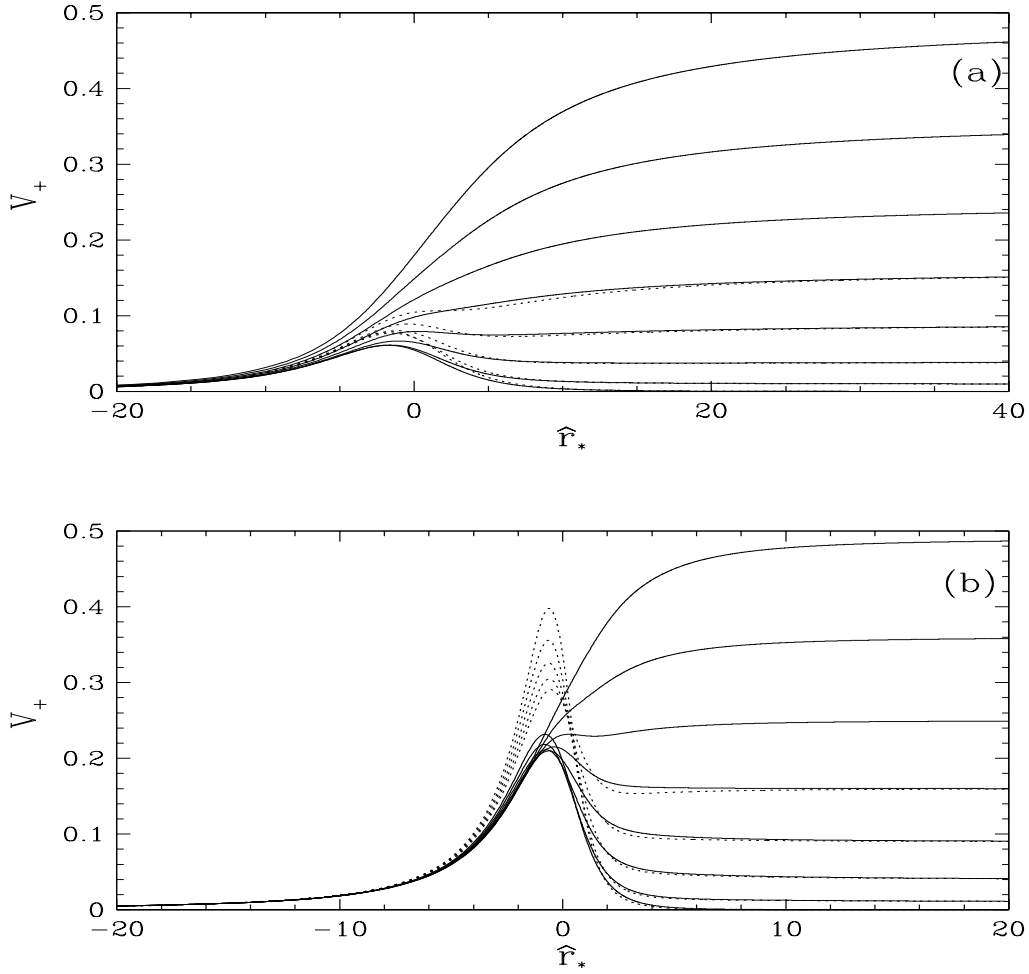

FIG. 10. Variation of V_+ as a function of $\hat{r}_*$, when (a) $a = 0.998$, $l = 0$, $M = 1$ (Kerr) (b) $a = l = 0.998$, $M = 0$ (dual Kerr). Solid curves are from top to bottom for $\sigma = 0.7$; $m_p = 0.7, 0.6, 0.5, 0.4, 0.3, 0.2, 0.1, 0$ and dotted are for $\sigma = 0.4$; $m_p = 0.4, 0.3, 0.2, 0.1, 0$, and $m = -1/2$, $Q_* = 0$.

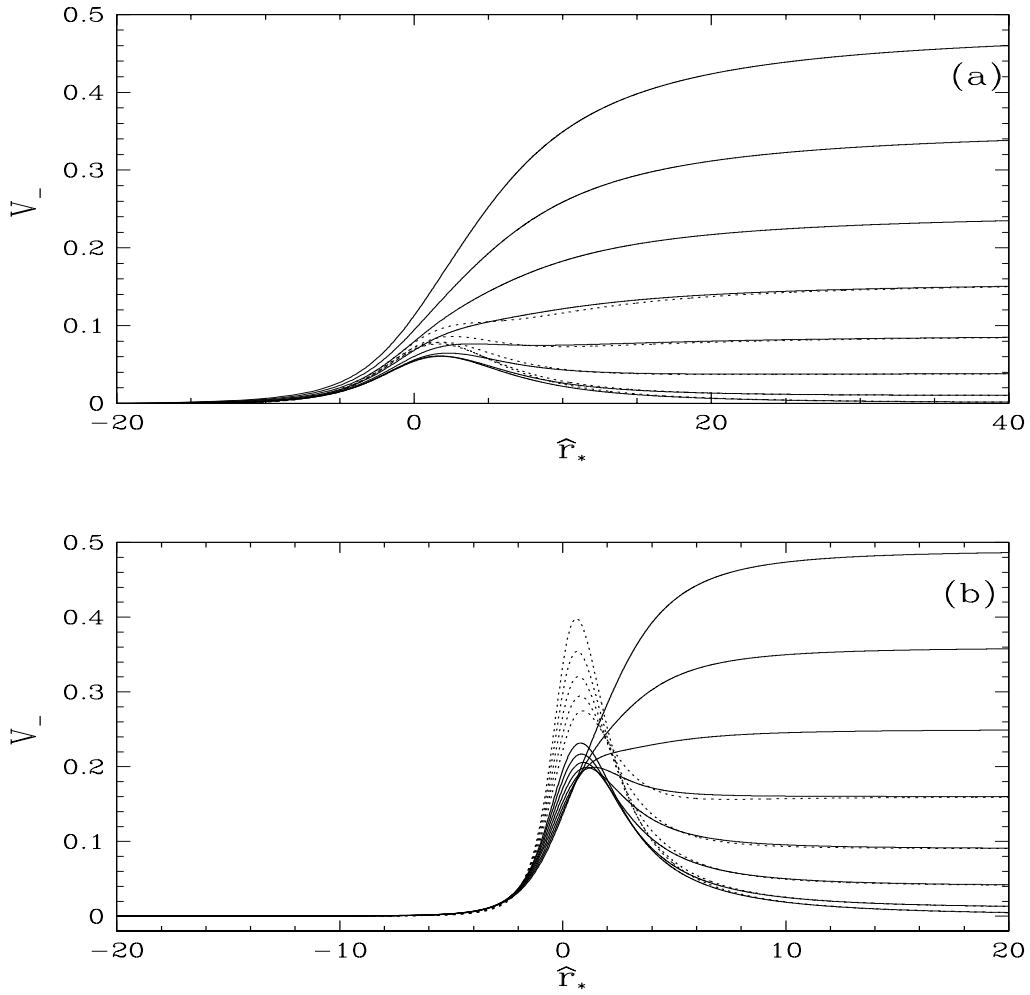

FIG. 11. Variation of V_{-} as a function of $\hat{r}_*$, when (a) $a = 0.998$, $l = 0$, $M = 1$ (Kerr) (b) $a = l = 0.998$, $M = 0$ (dual Kerr). Solid curves are from top to bottom for $\sigma = 0.7$; $m_p = 0.7, 0.6, 0.5, 0.4, 0.3, 0.2, 0.1, 0$ and dotted are for $\sigma = 0.4$; $m_p = 0.4, 0.3, 0.2, 0.1, 0$, and $m = -1/2$, $Q_* = 0$.

Therefore, from the above discussion we now have a clear picture of the behaviour of gravitational potential barriers felt by the spinors in the Kerr-NUT, Kerr and dual Kerr space-times. We will next study their solutions.

V. SOLUTION FOR SPINOR PERTURBATION

Here we like to solve Eqns. (36) and (40) for the various sets of the physical parameters. In view of the stationary and axisymmetric nature of the background space-time, it is natural to write the perturbation as superposition of waves of different modes, $exp[i(\sigma t + m\phi)]$. We have thus to solve the radial and angular equations. These equations are however not solvable analytically and hence we are forced to seek for numerical solutions. We shall employ the well known Runge-Kutta method with the boundary conditions at infinity. With the aim of getting the qualitative feeling of the solution, we shall again set $\lambda_2 = 1$, which should in principle be evaluated in an exact manner. The complete solution has been obtained for the Kerr geometry [17]. We shall however defer this for a future consideration for the Kerr-NUT geometry.

The numerical solutions are shown in the following figures. The boundary condition at infinity is fixed by demanding sinusoidal wave with the wave number, $k_{\pm} = \sqrt{\sigma^2 - V_{\pm}}$.

Figure 12 represents the behaviour of spinors in the angular direction for the Kerr-NUT and Kerr geometry. Recall from Figs. 3 and 4 that potential (which is also the square of wave number according to our notation) is positive only in the vicinity of $\theta = \pi/2$, then (36) can admit a harmonic oscillator like solution. We will essentially be interested in this region only because the regions of negative $W_{\pm}$ can only give exponentially increasing and/or decreasing solutions. The solutions clearly bring out the role played by the NUT parameter.

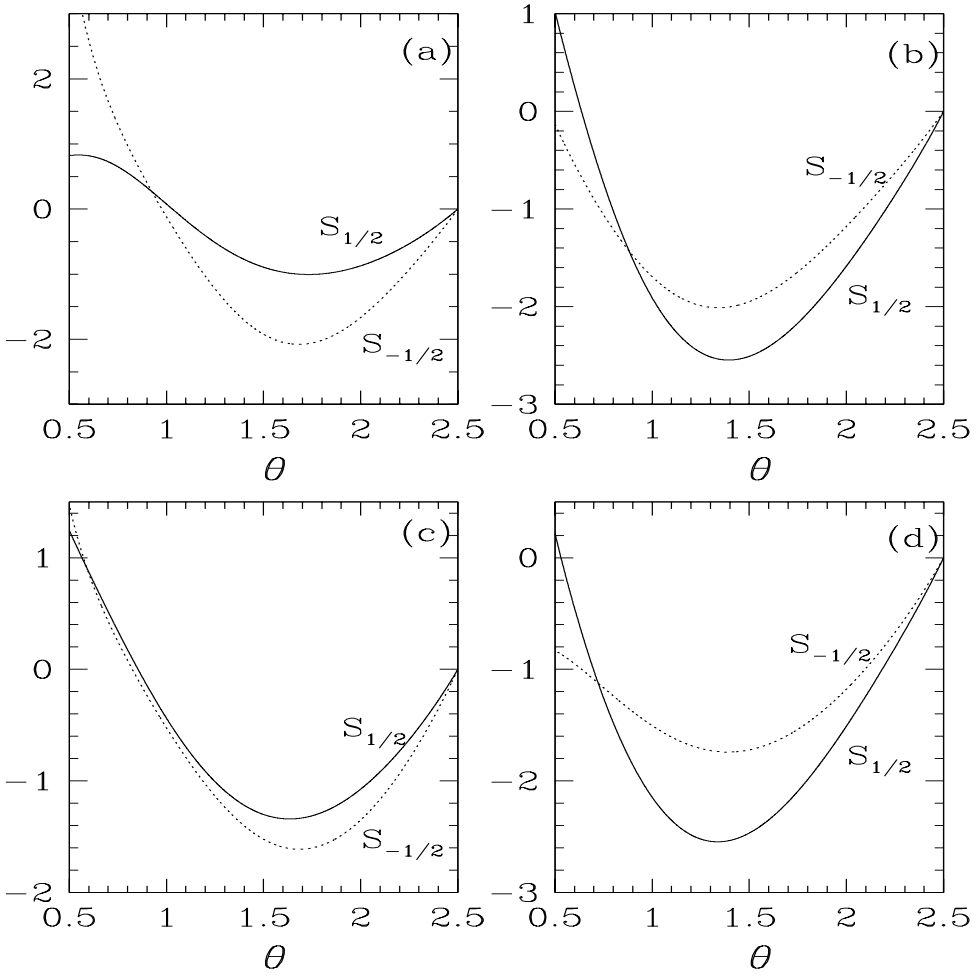

FIG. 12. Angular spin-up and spin-down solutions with $\sigma = m_p = 0.4$, for (a) Kerr-NUT, $a = 0.998$, $l = 0.99$ (b) Kerr, $a = 0.998$, (c) Kerr-NUT, $a = l = 0.5$, (d) Kerr, $a = 0.5$. Solid and dotted curves indicate the up and down spinors respectively as marked in the figure too. Other parameters are $m = -1/2$, $Q_* = 0$.

Figures 13 and 14 depict the corresponding radial evolution of spinors. The opposite sign of spin-spin coupling between the black hole and spinors of up and down alignment reflects into the solutions which show the amplitude of the spin down wave is significantly less compared to that of the spin up. The solutions in the dual Kerr (Fig. 13c) are shown in the semi-log scale just to catch the abrupt variations of curves as $r \to 0$ in the same plot extended upto a large r. At $r \to \infty$, $V_{\pm} \to m_p^2$, therefore the wave number of spinors becomes small at far away from the event

horizon which produces a large wavelength compared to that at a small r. For $\sigma = 0.4$, cases with $a = 0.5$ lie in the super-radiance regime for the dual Kerr and then the corresponding radial potentials diverge.

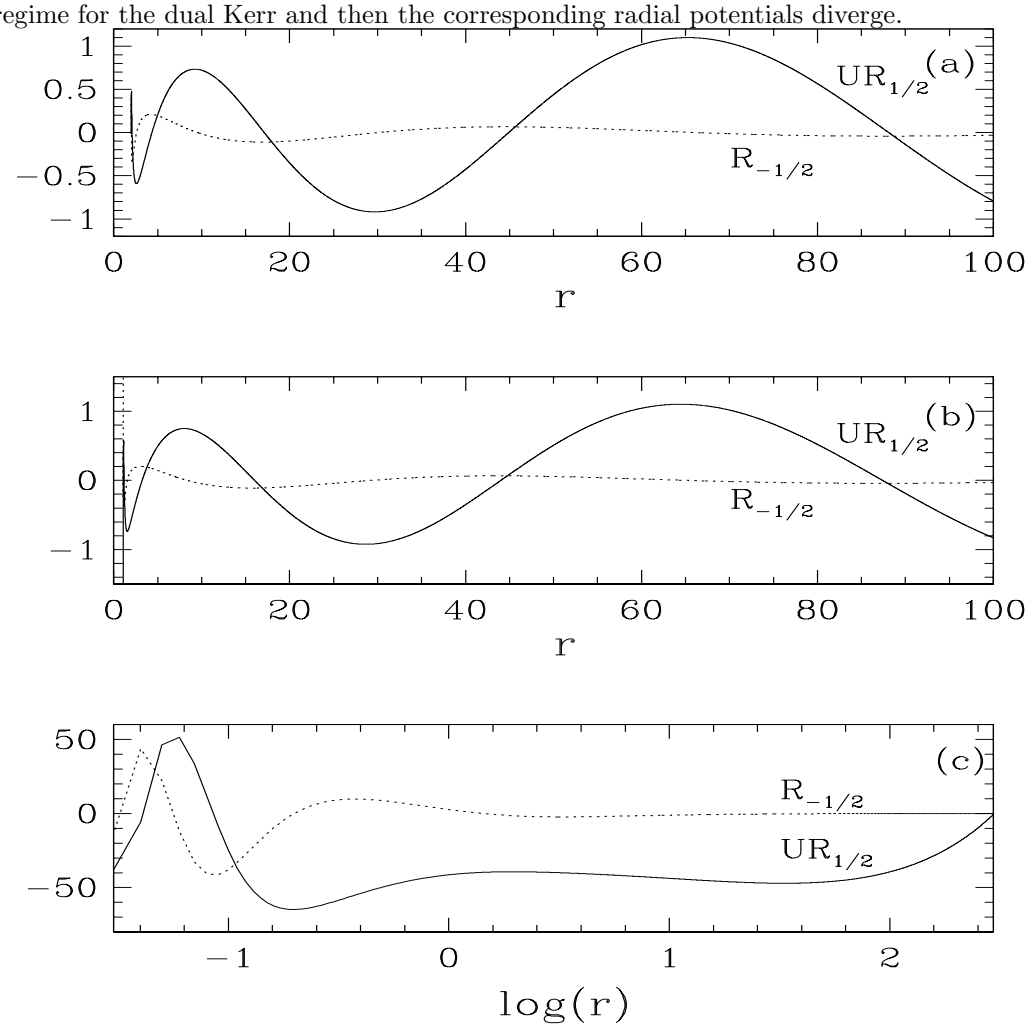

FIG. 13. Radial spin-up and spin-down solutions with $\sigma = m_p = 0.4$, for (a) Kerr-NUT, $a = 0.998$, $l = 0.99$ (b) Kerr, $a = 0.998$, (c) dual Kerr, $a = l = 0.998$. Solid and dotted curves indicate the up and down spinors respectively as marked in the figure too. Other parameters are $m = -1/2$, $Q_* = 0$; for (a) and (b) $M = 1$.

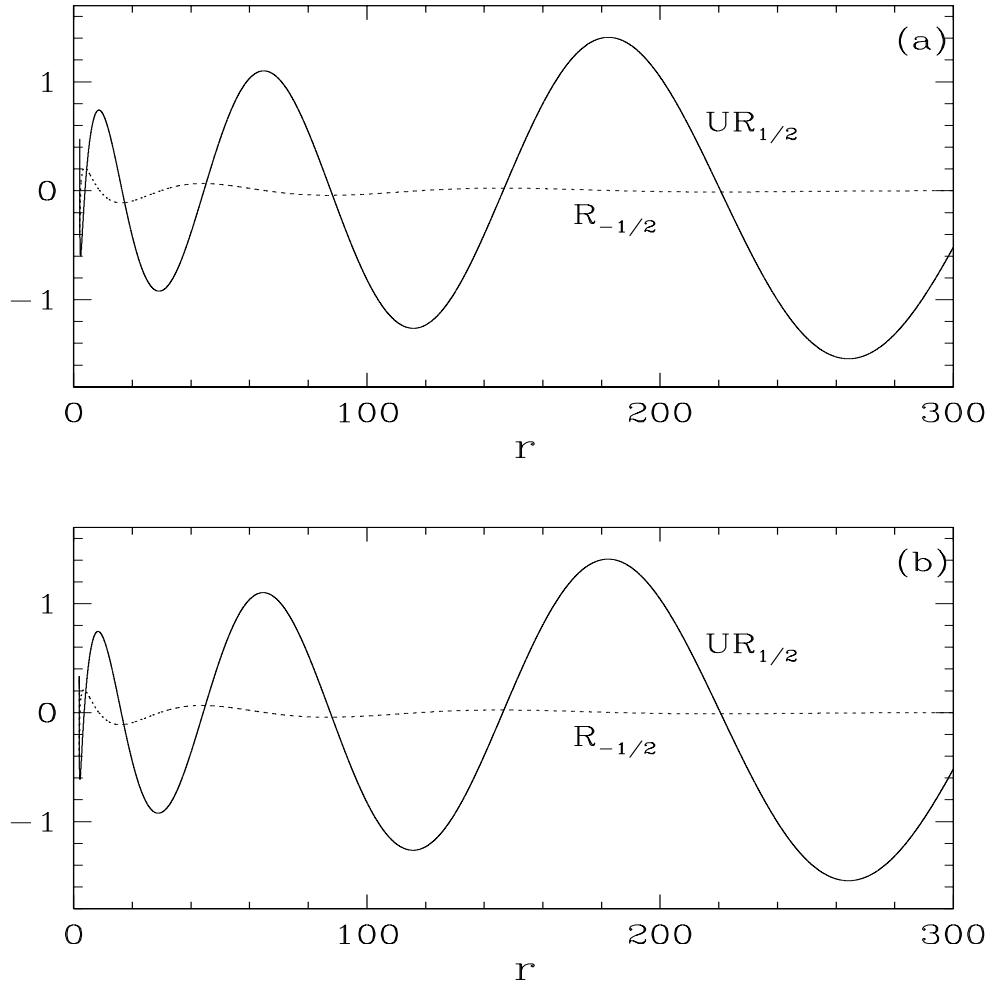

FIG. 14. Radial spin-up and spin-down solutions with $\sigma = m_p = 0.4$, for (a) Kerr-NUT, $a = l = 0.5$, (b) Kerr, $a = 0.5$. Solid and dotted curves indicate the up and down spinors respectively as marked in the figure too. Other parameters are $m = -1/2$, $Q_* = 0$, $M = 1$.

Now we will compare the solutions of the spinor perturbation equations in the various regimes of incoming spinors so that the black hole will appear to act as a mass-spectrograph. Figures 15 and 16 bring this feature for the angular up and down spinors respectively. As before only that range of θ is chosen when the solution is harmonic and it however covers most of the range of θ. The deviation of solutions for different sets of $\{\sigma, m_p\}$ is very clearly shown in the figures for the Kerr and Kerr-NUT space-times.

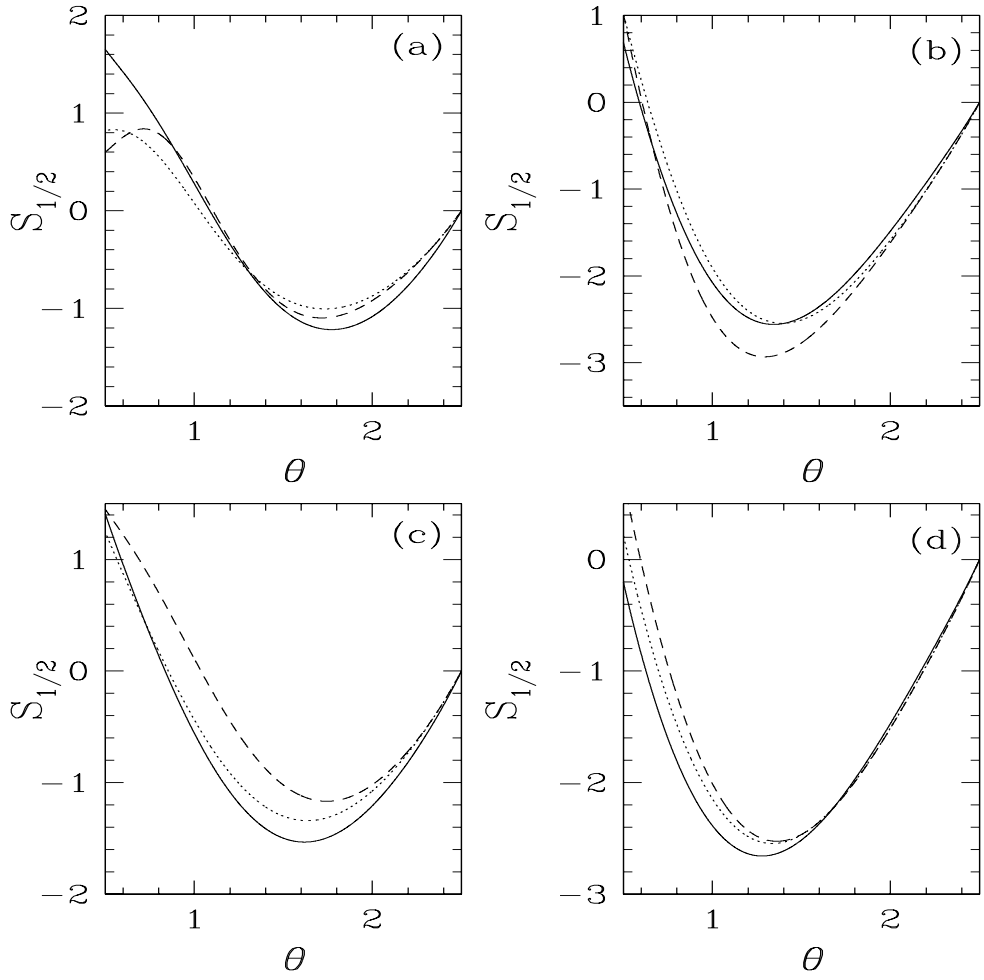

FIG. 15. Angular spin-up solutions with $\sigma = 0.4$, $m_p = 0.1$ (solid curve); $\sigma = 0.4$, $m_p = 0.4$ (dotted curve); $\sigma = 0.7$, $m_p = 0.4$ (dashed curve); for (a) Kerr-NUT, $a = 0.998$, $l = 0.99$, (b) Kerr, $a = 0.998$, (c) Kerr-NUT, $a = l = 0.5$, (d) Kerr, $a = 0.5$. Other parameters are $m = -1/2$, $Q_* = 0$.

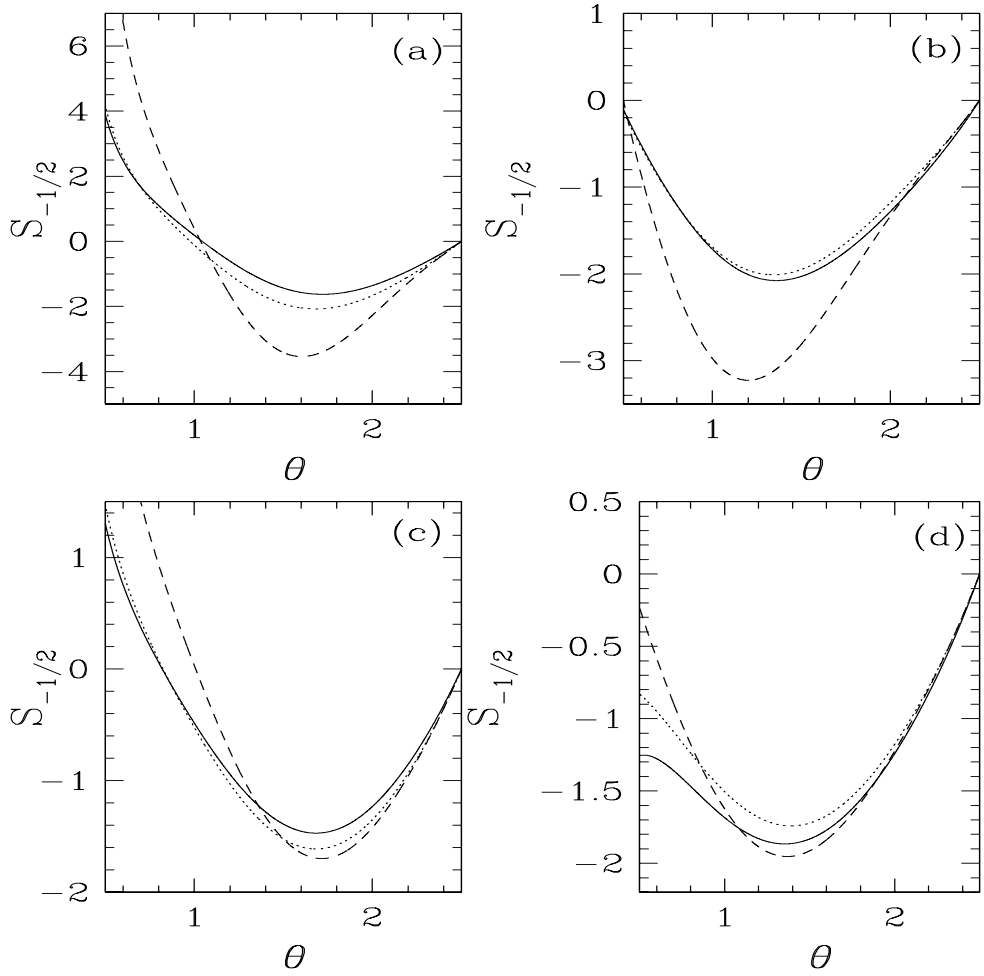

FIG. 16. Angular spin-down solutions with $\sigma = 0.4$, $m_p = 0.1$ (solid curve); $\sigma = 0.4$, $m_p = 0.4$ (dotted curve); $\sigma = 0.7$, $m_p = 0.4$ (dashed curve); for (a) Kerr-NUT, $a = 0.998$, $l = 0.99$, (b) Kerr, $a = 0.998$, (c) Kerr-NUT, $a = l = 0.5$, (d) Kerr, $a = 0.5$. Other parameters are $m = -1/2$, $Q_* = 0$.

Figures 17 and 18 indicate the solutions for the up and down spinors respectively in the radial direction in case of the extreme Kerr-NUT, Kerr and dual Kerr space-times for different choices of $\{\sigma, m_p\}$. The most interesting fact in all the figures is that when $\sigma \sim m_p$ (dotted curves) the wavelength as well as the amplitude of the spinors are high compared to two other cases. This is physically understood as $\sigma \sim m_p$ indicates the very small wave number at least at a large distance, that trend continues up to the inner radii, except at very close to the horizon where the strong effect of a black hole suppresses any individual identity of the matter. For $\sigma > m_p$, the perturbation of higher frequency gives rise to the solution of lower wavelength which is physically understood. Again the solutions for the dual Kerr are distinctly different from others. As before the overall amplitudes of up spinors which are oriented with the black hole's spin in a parallel sense, are high compared to that of down spinors oriented in an anti-parallel sense.

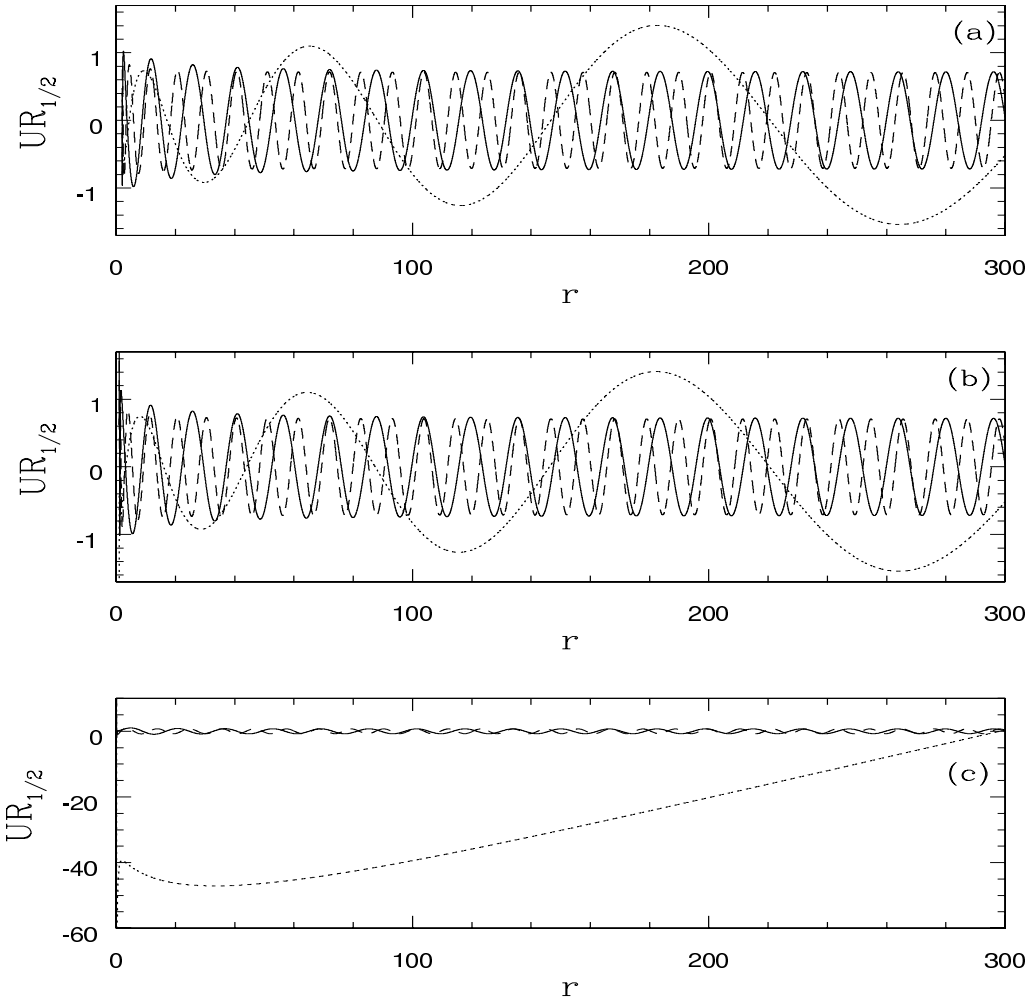

FIG. 17. Radial spin-up solutions with $\sigma = 0.4, m_p = 0.1$ (solid curve); $\sigma = 0.4, m_p = 0.4$ (dotted curve); $\sigma = 0.7, m_p = 0.4$ (dashed curve); for (a) Kerr-NUT, $a = 0.998$, $l = 0.99$ (b) Kerr, $a = 0.998$, (c) dual Kerr, $a = l = 0.998$. Other parameters are $m = -1/2$, $Q_* = 0$; for (a) and (b) $M = 1$.

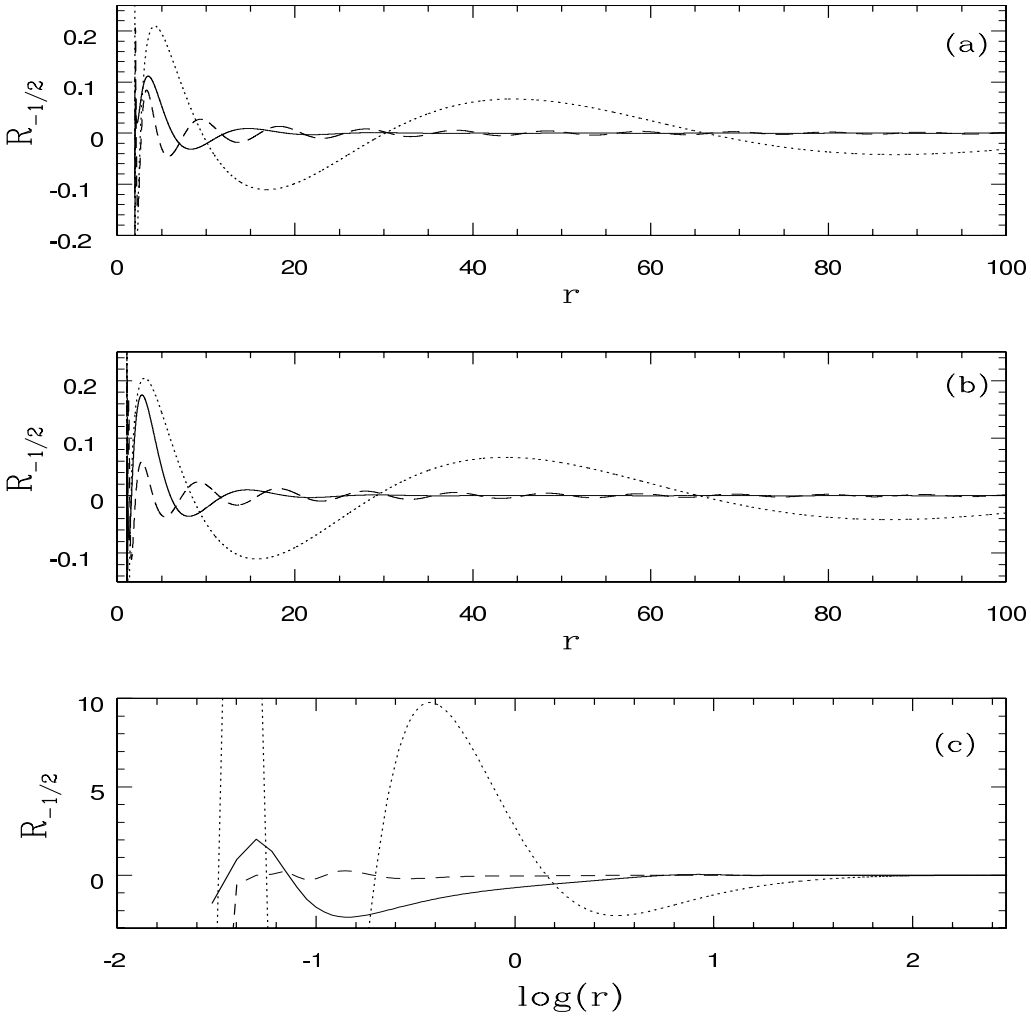

FIG. 18. Radial spin-down solutions with $\sigma = 0.4, m_p = 0.1$ (solid curve); $\sigma = 0.4, m_p = 0.4$ (dotted curve); $\sigma = 0.7, m_p = 0.4$ (dashed curve); for (a) Kerr-NUT, $a = 0.998$, $l = 0.99$ (b) Kerr, $a = 0.998$, (c) dual Kerr, $a = l = 0.998$. Other parameters are $m = -1/2$, $Q_* = 0$; for (a) and (b) $M = 1$.

The similar sets of solution are compared in Figs. 19 and 20 but for an intermediate rotating black hole. All the basic features are similar to that of Figs. 17 and 18 which are not repeated again. For the black hole angular momentum (Kerr parameter) $a = 0.5$ the corresponding $\sigma_s = 0.5$ in case of the dual Kerr with $l = 0.5$. Therefore only the $\sigma = 0.7$ case is out of the super-radiance regime and depicted in Figs. 19c and 20c.

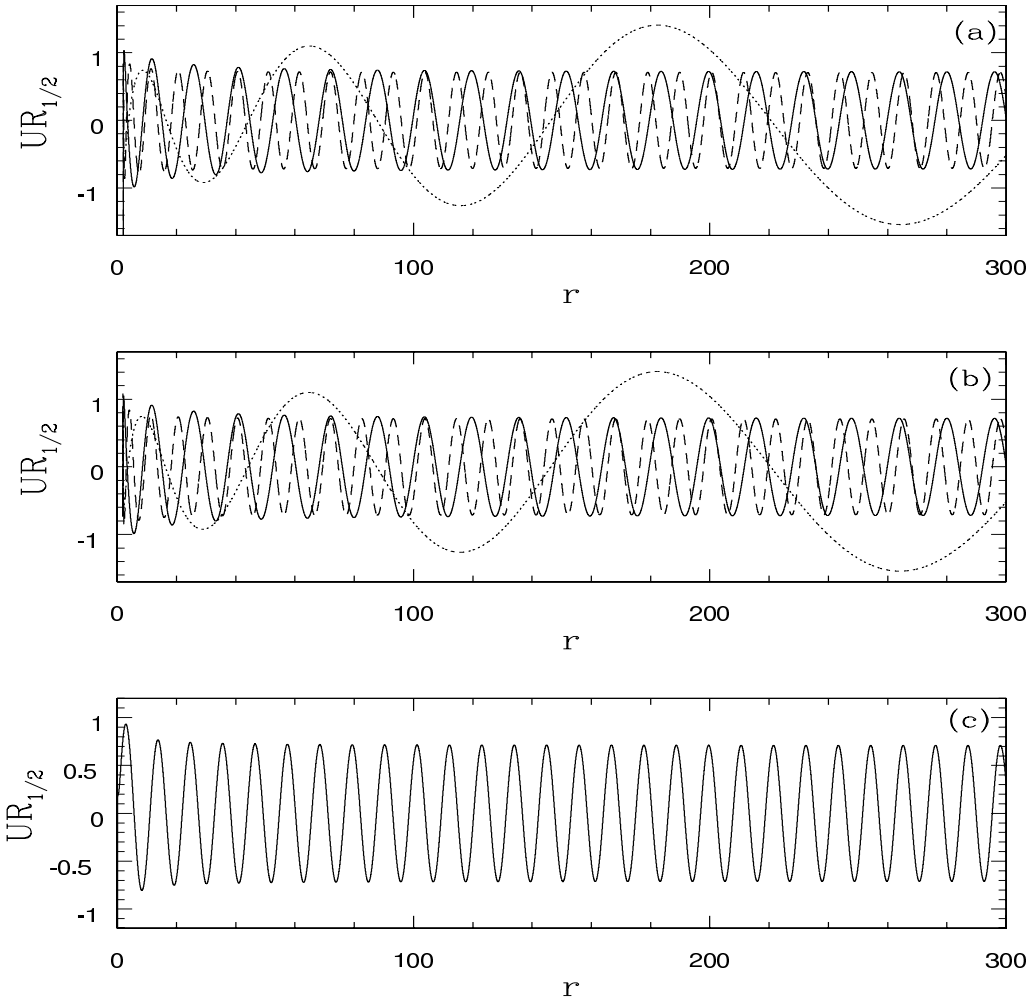

FIG. 19. Radial spin-up solutions with $\sigma = 0.4, m_p = 0.1$ (solid curve); $\sigma = 0.4, m_p = 0.4$ (dotted curve); $\sigma = 0.7, m_p = 0.4$ (dashed curve); for (a) Kerr-NUT, $a = l = 0.5$ (b) Kerr, $a = 0.5$, (c) dual Kerr, $a = l = 0.5$. Other parameters are $m = -1/2$, $Q_* = 0$; for (a) and (b) $M = 1$.

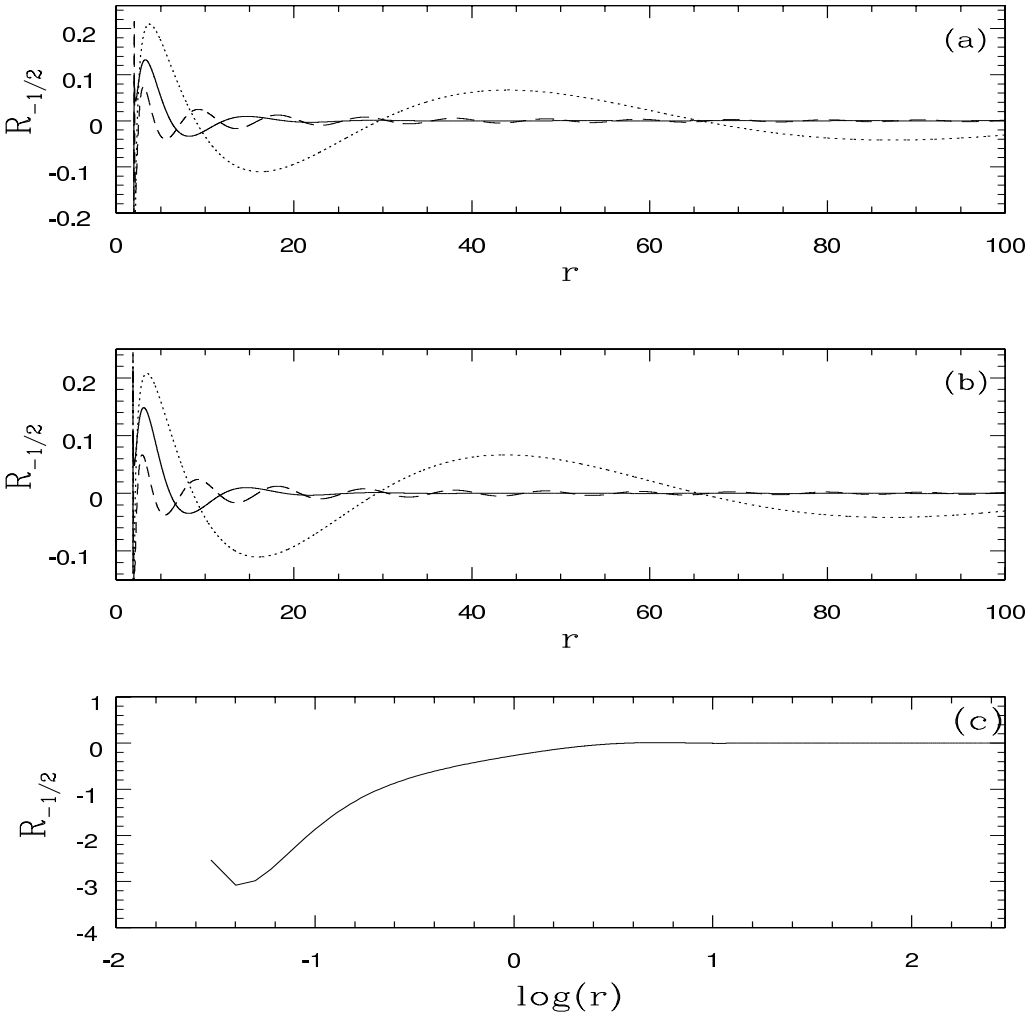

FIG. 20. Radial spin-down solutions with $\sigma = 0.4, m_p = 0.1$ (solid curve); $\sigma = 0.4, m_p = 0.4$ (dotted curve); $\sigma = 0.7, m_p = 0.4$ (dashed curve); for (a) Kerr-NUT, $a = l = 0.5$ (b) Kerr, $a = 0.5$, (c) dual Kerr, $a = l = 0.5$. Other parameters are $m = -1/2$, $Q_* = 0$; for (a) and (b) $M = 1$.

VI. HORIZON AND SINGULARITY

The distinguishing feature of the Kerr-NUT geometry is the presence of the magnetic charge which is called the NUT parameter, l, that causes the space-time to be asymptotically non-flat. The horizons are defined by $U = 0$ and hence they will occur at $r_\pm = M \pm \sqrt{M^2 + l^2 - a^2 - Q_*^2}$. We shall now switch off the electric charge, i.e. $Q_* = 0$, as it is not very pertinent to carry it through for the purpose in question. The singularity would occur where curvatures diverge and that would happen when $r^2 + (l + acos\theta)^2 = 0$. That means singularity would be located at $r = 0, cos\theta = -l/a$. Clearly there occurs no singularity when $l > a$. It is the ring like $(r = 0, \theta = \pi/2)$ for the Kerr case when $l = 0$ and string like when $a > l > 0$ (Kerr-NUT case). The string like character of the singularity is the characteristic of the presence of the NUT parameter [19].

On the other hand, horizon would always occur for $M^2 + l^2 \geq a^2$. For $l > a$, there occurs an interesting situation of having a horizon without singularity. The space-time is then non singular and regular everywhere. This is very strange because horizon should generally cover singularity. It has happened due to dominance of the NUT parameter

over the Kerr parameter. It is however well known that the NUT parameter also gives rise to the closed time-like geodesics. This suggests that the NUT parameter should never dominate over the Kerr parameter to ensure physical reasonableness.

If however, we wish to have the canonical picture of a black hole space-time having the horizon covering a singularity, then $l^2 < a^2$, which would imply $a \neq 0$ always. Recall that this was also required for the duality transformation between the electric (mass) and magnetic (NUT) charge. In case of the dual Kerr solution $M = 0$ and the horizon would be given by $r = \pm\sqrt{l^2 - a^2}$ which would require $l^2 \geq a^2$, while existence of singularity would require $l^2 \leq a^2$. Requiring both the horizon and singularity to coexist, we are unambiguously led to $l^2 = a^2$. The horizon occurs at $r = 0$ and it becomes singular when $\theta = 0, \pi$. The dual Kerr solution may not be very realistic but it provides an interesting vacuum space-time which is free of the usual electric gravitational charge (mass). The most remarkable feature is that general relativity admits a truly gravitational dyon solution which has the magnetic limit as the dual Kerr solution.

VII. DISCUSSION

We have studied the scalar and spinor perturbation in the Kerr-NUT (which includes the Kerr and dual Kerr) space-time which describe gravitational field of a rotating gravitational dyon with electric and magnetic charge. It is known that the Kerr-NUT space-time is invariant under the duality transformation which exchanges mass and NUT parameters as well as radial and angle coordinates [5,6]. By the duality transformation one can go from the Kerr to the dual Kerr solution and the vice versa. Interestingly, this duality transformation requires the rotation parameter to be non zero. Here we have shown that the same is true for the Klein-Gordon and Dirac equations in the Kerr-NUT space-time. That is, they are invariant under the duality, and they transform from the Kerr background to the dual Kerr, and the vice versa under the duality transformation with some appropriate rescaling of parameters.

In the Kerr geometry, angular part of the equation is free from mass and simply involves the kinematic aspects arising from rotation. With the NUT parameter, angular part attains active dynamical meaning by its presence. The radial part would however involve both the mass and NUT parameters. The behaviour of potentials and their solutions in different cases are shown in various figures. Potential barriers are higher for the dual Kerr space-time. This is because of the absence of mass, which produces the usual $1/r$ attractive potential while the NUT parameter, l, contributes $1/r^2$ asymptotically. Thus gravity is as expected stronger for the Kerr than the dual Kerr.

Though the Klein-Gordon and Dirac equations could be transformed under the duality transformation from the Kerr to the dual Kerr case, their solutions could not be transformed into each other by any simple duality transformation. Had the duality worked for the solutions of the equations, it would have indicated something profound. The problem is that in the Kerr background $l = 0$ while for the dual Kerr $M = 0$, the character of the equation changes drastically in the two cases and hence their solutions can not be related by the duality transformation. This however does not rule out the possibility that there may occur some other transformation which may work with the solutions. Note that in obtaining the solutions in a known form, we have defined the new independent variables in a complicated form which does not let duality transformation work at the solution level. With a proper and suitable new definition, it may

be possible to relate the solutions by the duality transformation. This as well as finding the complete solution with λ_1, λ_2 properly determined (rather than the qualitative solutions as considered here) of the perturbation equation we leave for future study. But we do however believe that this would not significantly alter the qualitative character of the solutions.

ACKNOWLEDGMENTS

We thank the referees for the useful suggestions that have improved the presentation of this paper. One of the author (B.M.) acknowledges the partial support by NSF grant AST 0307433 and NASA grant NAG5-10780 to this work.

---

[1] S. Chandrasekhar, in *The Mathematical Theory Of Black Holes* (London: Clarendon Press, 1983).
[2] E. T. Newman, L. Tamburino & T. Unti, J. Math. Phys. **4**, 915 (1963).
[3] B. Carter, Comm. Math. Phys. **10**, 280 (1968).
[4] M. Demianski & E. T. Newman, Bull. Acad. Polon. Sci. **14**, 653 (1966).
[5] N. Dadhich & Z. Ya. Turakulov, Class. Quantum Grav. **19**, 2765 (2002).
[6] N. Dadhich & Z. Ya. Turakulov, Mod. Phys. Lett. **A 17**, 1091 (2002).
[7] D. Lynden-Bell & M. Nouri-Zonoz, Rev. Mod. Phys. **70**, 427 (1998).
[8] N. Dadhich & L. K. Patel, J. Math. Phys. **41**, 882 (2000).
[9] Z. Ya. Turakulov & N. Dadhich, Mod. Phys. Lett. **A 16**, 1959 (2002).
[10] S. Teukolsky, Phys. Rev. Lett. **29**, 1114 (1972).
[11] S. Chandrasekhar, Proc. Roy. Soc. Lond. **A 349**, 571 (1976).
[12] B. Mukhopadhyay & S. K. Chakrabarti, Class. Quantum Grav. **16**, 3165 (1999).
[13] B. Mukhopadhyay & S. K. Chakrabarti, Nucl. Phys. **B 582**, 627 (2000).
[14] B. Mukhopadhyay, Class. Quantum Grav. **17**, 2017 (2000).
[15] W. H. Press & S. Teukolsky, Astrophys. J. **185**, 649 (1973).
[16] S. Teukolsky & W. H. Press, Astrophys. J. **193**, 443 (1974).
[17] S. K. Chakrabarti, Proc. Roy. Soc. Lond. **A 391**, 27 (1984).
[18] S. M. Wagh & N. Dadhich, Phys. Rev. **D 32**, 1863 (1985).
[19] J. Samuel & B. R. Iyer, Current Science **55**, 818 (1986).